

AperTO - Archivio Istituzionale Open Access dell'Università di Torino

Social behavior-induced multistability in minimal competitive ecosystems

This is a pre print version of the following article:

Original Citation:

Availability:

This version is available <http://hdl.handle.net/2318/1692941> since 2019-02-18T11:39:40Z

Published version:

DOI:10.1016/j.jtbi.2017.11.016

Terms of use:

Open Access

Anyone can freely access the full text of works made available as "Open Access". Works made available under a Creative Commons license can be used according to the terms and conditions of said license. Use of all other works requires consent of the right holder (author or publisher) if not exempted from copyright protection by the applicable law.

(Article begins on next page)

See discussions, stats, and author profiles for this publication at: <https://www.researchgate.net/publication/321181188>

Social behavior-induced multistability in minimal competitive ecosystems

Article in *Journal of Theoretical Biology* · November 2017

DOI: 10.1016/j.jtbi.2017.11.016

CITATIONS

4

READS

202

5 authors, including:



Chiara Perri

Università degli Studi di Torino

2 PUBLICATIONS 7 CITATIONS

[SEE PROFILE](#)



Malay Banerjee

Indian Institute of Technology Kanpur

130 PUBLICATIONS 1,664 CITATIONS

[SEE PROFILE](#)



Ezio Venturino

Università degli Studi di Torino

271 PUBLICATIONS 2,664 CITATIONS

[SEE PROFILE](#)

Some of the authors of this publication are also working on these related projects:



Mathematical/Theoretical Ecology [View project](#)



Modeling the effect of nutrient in plant disease [View project](#)

Social behavior-induced multistability in minimal competitive ecosystems

D. Melchionda[†], E. Pastacaldi[†], C. Perri[†], M. Banerjee^{‡*}, E. Venturino[†]

[†]Dipartimento di Matematica “Giuseppe Peano” via Carlo Alberto 10,
Università di Torino, 10123 Torino, Italy

[‡]Department of Mathematics & Statistics, IIT Kanpur, India

Abstract

Mimimal models of coordinated behavior of populations living in the same environment are introduced for the cases when they either both gain by mutual interactions, or one hunts the other one, or finally when they compete with each other. The equilibria of the systems are analysed, showing that in some cases the populations may both disappear. Coexistence leads to global asymptotic stability for symbiotic populations, or to Hopf bifurcations for predator-prey systems. Finally, a new very interesting phenomenon is discovered in the competition case: tristability may be achieved showing that the principle of competitive exclusion fails in this case. Indeed either one of the competing populations may thrive, but also the case of populations coexistence is allowed, for the same set of parameter values.

Keywords: predator-prey; symbiosis; competitive exclusion; group gathering; tristability; ecosystems.

AMS subject classification: 92D25, 92D40

1 Introduction

In the almost one-century-long history of mathematical modeling of population interactions, mostly their individualistic behavior has been taken into account. Only relatively recently the effect of group defense has been explicitly modeled, [15]. A slightly different concept is herd behavior, introduced in [1]. In this paper we extend it to encompass more general situations. We consider minimal models for two populations whose intermingling may be beneficial to both of them, beneficial for one and detrimental for the other one, or harmful for both of them. The classical models always assume individualistic behavior of each population, see e.g. Part I of [24]. Here, we remove this assumption by rather using the recently introduced concepts for mimicking the herd

*Corresponding author. E-mail: malayb@iitk.ac.in

26 group gathering of herbivores. In fact new models of such type have been considered in [1] and in
27 several other following papers e.g. [3, 4, 5, 23]. These differ quite a bit from other earlier ideas
28 relying on different assumptions on the shape of the functional response, [15], or from more recent
29 contributions, [16], in which starting from first principles and using the Becker and Döring equa-
30 tions for group size dynamics, a functional response similar to Holling type II (HTII) is derived for
31 the predators, although individuals follow a Holling type I (HTI) dynamics. The biological litera-
32 ture abounds on social, herd or pack behaviour, using concepts modeled via different mathematical
33 tools, e.g. graph theory or game theory, see for instance [17, 31] and the wealth of literature that is
34 cited in these papers. In the framework of animals' socialized behavior these ideas have recently
35 been discussed also in [3] and carried over to ecoepidemic systems in which the disease affects the
36 predators, [18], or considering several possibilities for the infected prey, that they may remain in
37 the herd or be left behind, [8, 22].

38 In this paper we confine ourselves only to the pure demographic situation, i.e. to models in the
39 absence of the disease. The basic picture is herbivores that gather in a herd and wander grazing
40 grass, assumed to be always available; when it becomes scarce, the herd moves to more favorable
41 pastures. When predators are considered, we assume them also to gather in a pack, follow the
42 herbivores and hunt them in a coordinate fashion. At the individual level, each individual competes
43 with its similars for space, as the resource is assumed, as said above, always available. Thus, the
44 logistic form for the population growth is a suitable assumption. At the population level, the
45 interaction is assumed to occur, again on a one-to-one basis, only among the individuals in the two
46 populations that occupy the outermost positions in each group. This is the basic distinctive feature
47 of the models introduced in this paper, with respect to [1, 8, 18, 33]. In these former studies, in
48 fact, only one of the two interacting populations gathers in a herd, while the other one behaves
49 individualistically.

50 We consider two populations, each forming a group, that interact in various ways. In particular,
51 for the predator-prey case, when the predators' pack hunts the prey some individuals generally have
52 a larger benefit. They are those that either take the best (social) positions because they are stronger
53 and therefore attack the prey before the other ones, obtaining a better gain, or simply those that
54 get the most advantageous (spatial) positions in the community in order to get the best share of
55 the prey. We assume therefore that in such case positions on the boundary of the pack have the
56 best returns for the individuals that occupy them, since they are the first to fall upon the prey. The
57 main idea of community behaviors for predators had been considered in [12]. Various forms of
58 functional responses are derived corresponding to different assumptions in the hunting behavior,
59 e.g. a ratio-dependent response function is obtained when predators are localized, i.e. the geometry
60 of the pack is not changed by adding more predators to it. On the other hand, the Hassell-Varley
61 function, [21], is obtained if the prey are captured in proportion to the area swept by the pack,
62 which depends on its front section.

63 In the present investigation, when a predator-prey interaction is considered, we examine two
64 situations for the prey, namely when they behave individualistically or when they gather in herds,
65 following the assumptions of [1]. In the latter situation, the most harmed prey during predators'
66 hunting are those staying on the boundary of the herd.

67 Here however we also extend the concept of group gathering to more general types of interac-

68 tions among populations thriving in the same environment. The cases of symbiosis and competition
69 are also well-known in the literature, for the Lotka-Volterra competition system in particular see
70 [34]. Again, the classical approach, in which both populations behave individually, will be
71 replaced by more social attitudes, such as herd or pack behavior. In part this idea has been intro-
72 duced in [1], but assuming that only one population behaves socially, the individuals of the other
73 one live independently of each other. Thus, we extend now the analysis to the case in which both
74 populations show a community behavior, both when each one of the two communities benefits
75 from the interactions with the other one, as well as to the case in which the communities compete
76 with each other. More specific ecological examples will be discussed below.

77 The systems introduced here are intended to be minimal, in order to emphasize their outcomes
78 due to the specific herd behavior assumptions made. In this idealized setting, the interactions oc-
79 curring on the edge of the pack are mathematically modeled via suitable nonlinear functions of the
80 populations. These nonlinearities are purposely chosen to replace the classical terms coming from
81 the mass action law, containing products of the two populations. These nonlinearities represented
82 by Gompertz-like interaction terms, i.e. terms in which the populations appear raised to a fixed ex-
83 ponent, whose value is $\frac{1}{2}$. This value comes from its geometric meaning, it represents the fact that
84 the perimeter of the patch occupied by the population is one-dimensional, while the patch itself is
85 two-dimensional, as explained in detail below.

86 The basic ideas underlying modeling herd behavior have been expounded in [1]. For the benefit
87 of the reader we recall here the main steps. Consider a population that gathers together. Let P
88 represent its size. If this population occupies a certain territory of size A , the number of individuals
89 staying at the outskirts of the group, be it the pack or the herd, is directly related to the length of
90 the perimeter of the territory occupied by the herd. Therefore its length is proportional to \sqrt{A} . We
91 take the population P to be homogeneously distributed over the two-dimensional domain A . Thus
92 its square root, i.e. \sqrt{P} will count the individuals on the perimeter of the territory.

93 Let us assume that another population Q intermingles with the one just considered. At first,
94 assume that Q behaves individually, the individuals do not gather in a group. We assume
95 that the interactions of the latter with the former population occur mainly via the individuals in it
96 living at the periphery, which are proportional to \sqrt{P} , as mentioned. Thus the interaction terms in
97 this case are proportional to $Q\sqrt{P}$.

98 Instead let us now assume that the second population Q gathers in a group and intermingles with
99 P . Assuming again that the interactions of the two populations occur mainly via the individuals
100 living at the periphery, in this case the interaction terms must be proportional to the subsets of the
101 two populations on the edge of their respective groups and therefore will contain square root terms
102 for both populations. They will thus be modeled via $\sqrt{Q}\sqrt{P}$.

103 Further, interactions between population can be of different types. They can benefit both, in
104 the case of symbiosis. Alternatively they can damage both populations, when they compete among
105 themselves directly or for common resources. Finally, one population receives an advantage at
106 the expense of the other one; this happens in the predator-prey situation. As a consequence, note
107 that these mathematical differences involve sign changes in the corresponding interaction terms.
108 With the exception that involves pack predation and individual prey, not considered in [1], we will
109 concentrate on models involving both populations with individuals sticking together. In the models

110 under scrutiny in this paper, we keep the biological setting to a minimum, in order to highlight the
111 differences that this formulation entails with respect to the classical one-to-one interaction models.

112 To better ecologically motivate the models, we illustrate here some possible biological exam-
113 ples for each envisaged situation.

114 For the predator-prey case a simple example of the two possible demographic interactions is
115 provided by wolves (*Canis lupus*) or other carnivores hunting in packs either isolated prey or herds
116 of herbivores.

117 The symbiotic case can be illustrated in several ways. There are several associations between
118 populations that are beneficial to both, or beneficial to one and neutral for the other one. For
119 instance, in the roots of legumes, diverse microbiomes, rhizobia, nitrogen-fixing bacteria are found,
120 while in alder root nodules thrive actinomycete nitrogen-fixing Frankia bacteria, [27], [29] p. 142,
121 so that, mainly producing malate and succinate dicarboxylic acids, photosynthesis can occur. Fungi
122 can penetrate the cortex cells of the plant's secondary roots, thereby forming an association named
123 mycorrhiza. Most of land ecosystems depend on the beneficial associations between mycorrhizal
124 fungi, that extract minerals, inorganic nitrogen and phosphorus, from the ground and the plants,
125 fixing carbon from the air, [20]. The fungi may also secrete antibiotics thereby protecting the
126 host plant from parasitic fungi and bacteria. It is well known, [30], that symbiotic relationships
127 among fungi in arbuscular mycorrhizas involve about 80% of the plants. Note that we mention
128 this example in spite of the fact that it represents a three-dimensional structure. It therefore would
129 require a modification of the square root term in our model, which would become the power $2/3$.
130 Indeed this is the ratio of surface area to volume in a three-dimensional situation and would replace
131 the ratio perimeter to area of the two-dimensional case. In a very recent investigation, this problem
132 has been addressed in its full generality, [6], allowing for a general exponent α encompassing
133 also possible fractal domains. Although we could also consider the general situation in this paper,
134 however, we prefer to address the square root situation only, to better illustrate the ecological
135 implications without obscuring them with more complicated mathematics.

136 Another instance of association beneficial to both populations is provided by bullhorn acacia
137 trees harboring stinging ants among their thorns. The acacia tree provides the ants with food, its
138 very sweet nectar exuding from nectaries, its specialized structures, and the Beltian bodies,
139 food nodules growing on the leaves. Ants in turn attack anything approaching the perimeter of
140 their host, even killing branches of neighboring trees and removing all the vegetation around their
141 tree's trunk. Epiphytes, like orchids and other members of the pineapple family, thrive on the edge
142 of stronger plants gaining better sunlight exposure, but do not assume nourishment from their host.

143 In the marine world finally, the mollusc *Elysia viridis* (Mollusca) hosts the endosymbiont
144 *Codium fragile*, that produces Photosynthates, while obtaining protection and inorganic nutrients,
145 [32].

146 In all these examples, note that the interactions occur on the perimeter of the occupied areas
147 of each population, or through the surface of their leaves or roots. It makes therefore sense to
148 investigate these population interactions via square root terms as explained above.

149 For the case of competing populations, an example of this situation is provided by herbivores
150 sharing, or better, competing, for grass in high pastures. In the Alps, during the summer season
151 domestic animals like goats and cows are brought into the high pastures for feeding. These herds

152 become in close contact, but do not intermingle, with the wild herds of chamoises (*Rupicapra r.*
153 *rupicapra*) and ibexes (*Capra i. ibex*). Thus the interactions among domestic goats and cows with
154 wild herbivores, occurring at the edge of the respective herds, has negative consequences for both,
155 as food is subtracted from one population to the other one, and vice versa. Note that the interactions
156 are really close, so that even diseases like infectious keratoconjunctivitis can be transmitted from
157 one herd to the other one, [25].

158 The paper is organized as follows. The next Section presents the two predator-prey cases. Sec-
159 tion 3 investigates the cases of symbiosis. Section 4 presents the competing populations, showing
160 new unexpected results with respect to the corresponding classical case. A final discussion con-
161 cludes the paper, comparing these findings with the classical models. The appendix contains the
162 mathematical preliminaries, the analysis of the system's equilibria and the investigation also of the
163 more complex behavior of these models.

164 To sum up, the novelty of this work lies in the study of predators' pack hunting of either indi-
165 vidual or herd-gathered prey, Both minimal models introduced in Section 2 are therefore new, in
166 view of the presence of the square root terms for the predators. For the symbiotic and competing
167 cases, again the models are new because they contain square root terms for both interaction terms.
168 The findings indicate an unexpected outcome for the competition, namely tristability, which is im-
169 possible for the classical case of 1-1 interactions among competing populations. This results shows
170 that the principle of competitive exclusion may not hold under these "peripheral interactions" as-
171 sumptions.

172 2 The predator-prey cases

173 In this section, we let $P(t)$ represent the predators and $Q(t)$ denote the prey populations as func-
174 tions of time t . There are two possible different situations that can arise, when predators hunt in a
175 coordinate fashion: the prey can either wander about in an isolated fashion, or can gather together
176 in herds.

177 In the two models that follow, the parameters bear the following meaning. The parameter r is
178 the net growth rate of the Q population, with K being its environment's carrying capacity. The
179 hunting rate on the prey is denoted by the parameter q , while p denotes its reward for the predators
180 and m is their natural death rate. The following systems will be considered, in which all the
181 parameters are assumed to be nonnegative.

182 First, the predator-prey interactions of pack-individualistic type, for a specialized predator

$$\frac{dQ}{dt} = r \left(1 - \frac{Q}{K}\right) Q - q\sqrt{P}Q, \quad \frac{dP}{dt} = -mP + p\sqrt{P}Q. \quad (2.1)$$

183 Secondly, the pack predation-herd behavior, system, for a specialized predator

$$\frac{dQ}{dt} = r \left(1 - \frac{Q}{K}\right) Q - q\sqrt{P}\sqrt{Q}, \quad \frac{dP}{dt} = -mP + p\sqrt{P}\sqrt{Q}. \quad (2.2)$$

184 Corresponding models for the case of generalist predators could be formulated, but are not consid-
185 ered here to reduce the length of the paper.

186 If one of the two populations disappears the system reduces to one equation. In this circum-
 187 stance if the prey survive, they follow a logistic growth toward their carrying capacity, while if
 188 they vanish, the predators cannot survive. In fact when $Q = 0$ the equation for the predators shows
 189 that they exponentially decay to zero. This makes sense biologically, since these are specialistic
 190 predators. Thus in these two models the disappearance of both populations is a possibility. The
 191 equilibrium corresponding to population's collapse is the origin. Its stability can be analysed by a
 192 simple expansion of the governing equations near zero, keeping only the dominant terms.

The predator-prey case (2.1) leads to

$$\frac{dQ}{dt} \sim rQ > 0, \quad \frac{dP}{dt} \sim -mP < 0,$$

so that the origin is unstable. In the case (2.2) instead we find

$$\frac{dQ}{dt} \sim \sqrt{Q}(r\sqrt{Q} - q\sqrt{P}), \quad \frac{dP}{dt} \sim \sqrt{P}(-m\sqrt{P} + p\sqrt{Q})$$

193 and both populations under unfavorable circumstances may well disappear. This happens when

$$\frac{\sqrt{Q}}{\sqrt{P}} < \min \left\{ \frac{m}{p}, \frac{q}{r} \right\}. \quad (2.3)$$

194 2.1 Pack predation and individualistic prey behavior

195 We consider now (2.1). The following results hold. Their mathematical proofs are found in Ap-
 196 pendix **A1.1**. All positive solutions of (2.1) are forward bounded. Here the coexistence equilibrium
 197 $E_2^{[pi]}$ can be evaluated explicitly,

$$E_2^{[pi]} = \left(\frac{rmK}{rm + pqK}, \frac{r^2p^2K^2}{(rm + pqK)^2} \right), \quad (2.4)$$

198 is clearly always feasible and it is always locally asymptotically stable. Moreover, no persistent
 199 oscillatory behavior is allowed and as a further consequence the coexistence equilibrium must also
 200 be globally asymptotically stable. In summary, for strictly positive initial conditions, the ecosystem
 201 populations evolve necessarily to the values given by the coordinates of $E_2^{[pi]}$, independently of the
 202 state of the system that is considered as a starting value.

203 2.2 Pack predation and prey herd behavior

204 We focus now on (2.2), please refer to Appendix **A1.2** for more details. Once again, also in this
 205 case all positive solutions of (2.2) are forward bounded.

206 The coexistence equilibrium $E_2^{[ph]}$ has the following analytic representation

$$E_2^{[ph]} = \left(\frac{rm - pq}{rm} K, \frac{rm - pq}{rm^3} Kp^2 \right) \quad (2.5)$$

207 and it is feasible for

$$rm \geq pq. \quad (2.6)$$

208 When it is unfeasible, the origin is then the only possible equilibrium. Both populations vanish
 209 also when (2.6) becomes an equality. This is further asserted by recalling the fact that in the case
 210 of (2.2) the origin might indeed be achievable, (2.3). Note that when locally asymptotically stable,
 211 the origin is also globally asymptotically stable. In addition, there is a transcritical bifurcation for
 212 which $E_2^{[ph]}$ emanates from the equilibrium E_0 when the parameter r raises up to attain the critical
 213 value $r^* = pqm^{-1}$.

The coexistence equilibrium of the system (2.2) is locally asymptotically stable if (A.17) holds;
 in such case we must have

$$r > \max \left\{ m, \frac{3pq - m^2}{2m} \right\}.$$

But in the range

$$\frac{pq}{m} < r < \max \left\{ m, \frac{3pq - m^2}{2m} \right\}$$

214 we find that $E_2^{[ph]}$ is unstable. Furthermore, the ecosystem starts oscillating in a persistent manner
 215 around the coexistence equilibrium when the bifurcation parameter r crosses the critical value

$$r = r^\dagger = \frac{3pq - m^2}{2m}. \quad (2.7)$$

216 Figure 1 shows the limit cycles for the dimensionalized model (2.2), letting the simulation run for
 217 long times to show that the oscillations are indeed persistent, using the Matlab integration routine
 218 ode23t.

219 Finally, it is worthy to note an interesting phenomenon that hardly occurs in population models,
 220 that has already been remarked in [33, 18], namely the fact that the system (2.2) admits trajectories
 221 for which the prey go to extinction in finite time, if the initial conditions lie in the set

$$\Xi = \left\{ (Q, P) : P > 0, 1 \geq Q \geq \exp \left(-\frac{q}{r} \sqrt{P} \right) \right\}, \quad (2.8)$$

222 We summarize the equilibria of system (2.2) in the following table.

Parameter conditions	E_0	$E_2^{[ph]}$	Bifurcation
$r < \min \left\{ m, \frac{pq}{m} \right\}$	stable	unfeasible	
$r < m, \quad r^* = \frac{pq}{m}$			transcritical
$r > \max \left\{ m, \frac{3pq - m^2}{2m} \right\}$	unstable	stable	
$r > m, \quad r = r^\dagger = \frac{3pq - m^2}{2m}$			Hopf
$r > m \quad \frac{pq}{m} < r < \frac{3pq - m^2}{2m}$	unstable	unstable	
$r > m \quad \frac{3pq - m^2}{2m} > r$	unstable	unfeasible	

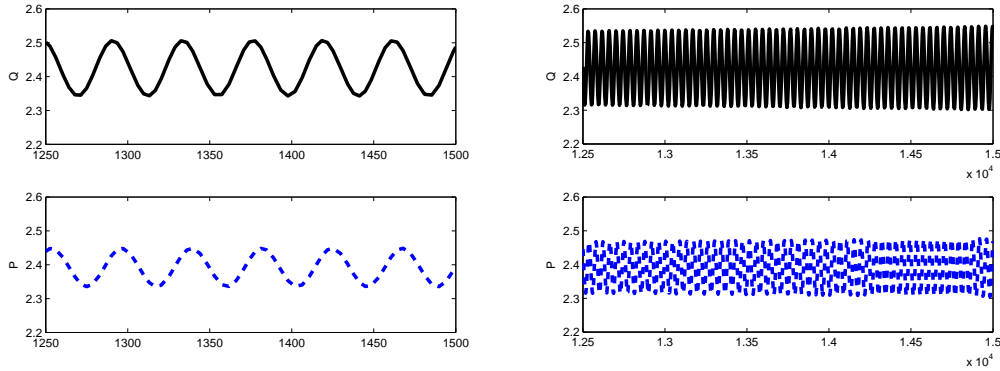


Figure 1: Left: time series of the system trajectories (2.2) up to $t = 1500$; Right: the same situation, but followed for a much longer time, up to $t = 15000$, to show that these are really persistent oscillations. The original parameter values are $r = 0.75937$, $m = 0.299$, $p = 0.297$, $q = 0.61$, $K = 12$; The initial condition is $(2.44, 2.36)$, with coexistence equilibrium $E_2^{[ph]} = (2.4253, 2.3930)$. With these values we obtain $e = 1.2698$ and $f = 0.5066$ so that we are above the dashed line, $e - 2f = 0.2566 > 0$ (coexistence feasibility), but below the continuous line, $0.25 + e - 3f = -1.605 \times 10^{-5} < 0$ (coexistence instability). The eigenvalues of the Jacobian at equilibrium, $0.48 \times 10^{-6} \pm 0.1515 i$, with positive real part, and the trace of the Jacobian $9.6 \times 10^{-6} > 0$, also positive, both show instability.

3 The symbiotic model

For the mathematical details of this section, please refer to Appendix A2. Let us denote by $P(t)$

and $Q(t)$ the sizes of two populations in consideration as functions of time t . The parameters r

227 and m are the growth rates respectively of the Q and P populations, with K_Q and K_P denoting
 228 their carrying capacities. Beneficial interaction rates between the two populations are denoted by
 229 the parameter q for the Q population and by p for the P 's. The following symbiotic system is
 230 considered, in which all the parameters are assumed to be nonnegative:

$$\frac{dQ}{dt} = r \left(1 - \frac{Q}{K_Q}\right) Q + q\sqrt{P}\sqrt{Q}, \quad \frac{dP}{dt} = m \left(1 - \frac{P}{K_P}\right) P + p\sqrt{P}\sqrt{Q}. \quad (3.1)$$

231 If one of the two populations disappears the system reduces to one equation and the surviving
 232 population tends to its own carrying capacity.

The equilibrium corresponding to both population's collapse is the origin. Its stability can be analysed by a simple expansion of the governing equations near zero, keeping only the dominant terms:

$$\frac{dQ}{dt} \sim \sqrt{Q}(r\sqrt{Q} + q\sqrt{P}) > 0, \quad \frac{dP}{dt} \sim \sqrt{P}(m\sqrt{P} + p\sqrt{Q}) > 0.$$

233 Thus both symbiotic populations cannot vanish.

234 The investigation of the coexistence equilibrium E_3^S of both populations shows that it results
 235 unconditionally feasible and the system trajectories remain forward bounded. Further, populations
 236 cannot exhibit persistent oscillations around this point, as Hopf bifurcations are shown never to
 237 arise, and the system trajectories remain forward bounded. These results imply also that the co-
 238 existence equilibrium is globally asymptotically stable. Summing up these considerations, in this
 239 case the ecosystem always evolves toward an equilibrium point at which both populations thrive,
 240 this being independent of its initial or present conditions.

241 4 The competition model

242 As for the symbiotic model let $P(t)$ and $Q(t)$ denote the populations of interest, r and m their net
 243 growth rates, K_Q and K_P their carrying capacities, q and p their competition rates. The competing
 244 model, where all the parameters are nonnegative, is

$$\frac{dQ}{dt} = r \left(1 - \frac{Q}{K_Q}\right) Q - q\sqrt{P}\sqrt{Q}, \quad \frac{dP}{dt} = m \left(1 - \frac{P}{K_P}\right) P - p\sqrt{P}\sqrt{Q}. \quad (4.1)$$

245 First of all, the model is ecologically well-posed in view of the fact that the positive solutions
 246 of (4.1) are forward bounded. Again the details are contained in Appendix A3.

Again, if one of the two populations disappears the surviving one grows logistically to its own carrying capacity. This ecosystem can also totally disappear, since the stability of the origin can be analysed by a simple expansion of the governing equations near zero, keeping only the dominant terms:

$$\frac{dQ}{dt} \sim \sqrt{Q}(r\sqrt{Q} - q\sqrt{P}), \quad \frac{dP}{dt} \sim \sqrt{P}(m\sqrt{P} - p\sqrt{Q}).$$

247 In this case both populations may disappear, when

$$\frac{m}{p} < \frac{\sqrt{Q}}{\sqrt{P}} < \frac{q}{r}. \quad (4.2)$$

248 The coexistence equilibria can be obtained as an intersection of cubic functions, shown in Fig-
 249 ure 2. Several outcomes are possible, giving rise in some cases to multiple equilibria. Specifically,
 250 if

$$pq > rm \quad (4.3)$$

251 no feasible coexistence equilibria exist. If

$$pq < rm \quad (4.4)$$

252 at least one feasible equilibrium exists, $E_3^C = (X_3^C, Y_3^C)$. Further, in such case, three equilibria
 253 may exist, i.e. E_4^C , E_3^C and E_5^C , ordered for increasing values of their abscissae. The sufficient
 254 conditions ensuring these three equilibria to exist are

$$\frac{m}{p} \frac{2}{3\sqrt{3}} > \frac{\sqrt{K_Q}}{\sqrt{K_P}} > \frac{q}{r} \frac{3\sqrt{3}}{2} \quad (4.5)$$

255 In addition, the equilibria for which either one of the conditions

$$Q < \frac{K_Q}{3}, \quad P < \frac{K_P}{3}, \quad (4.6)$$

256 hold are unstable.

257 Considering Figure 2, in the case of just one equilibrium, it must have at least one coordinate
 258 to the left (or below) the one of the local maximum of the function. In the plot, it has the abscissa
 259 smaller than the one of the local maximum of the parabola with vertical axis (i.e. the function
 260 $Y_{[1]}(X)$ given by (A.24) in Appendix A3). Thus when E_3^C is unique, it must be unstable. For the
 261 case of three equilibria, evidently E_4^C and E_5^C have either the abscissa (E_4^C) or the height (E_5^C)
 262 satisfying the corresponding condition in (4.6). Hence these two equilibria must be unstable as
 263 well.

264 In case of three equilibria, the system exhibits the following additional feature. The equilibrium
 265 E_3^C for which both the conditions

$$Q > \frac{K_Q}{3}, \quad P > \frac{K_P}{3}, \quad (4.7)$$

266 hold is locally asymptotically stable. There is a subcritical pitchfork bifurcation: from the unstable
 267 E_3^C three equilibria emanate, with the equilibrium E_3^C becoming stable and the other ones being
 268 unstable.

269 Finally, no persistent oscillations around the coexistence equilibrium can arise.

270 In Figure 3 we show the behavior of the two populations in the phase plane in each of the three
 271 possible cases.

272 4.1 Bifurcations

273 In this section we describe the possible local bifurcations that can take place for the appearance
 274 and disappearance of interior equilibrium points through two types of local bifurcations, namely

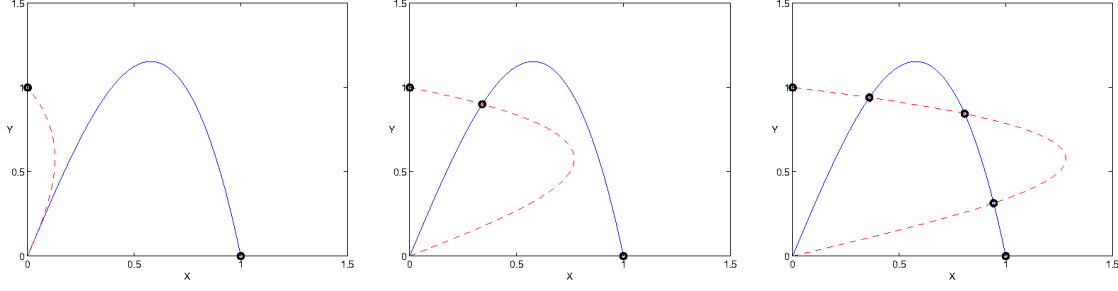


Figure 2: Referring also to Figure 12, we show here the coexistence equilibria possible scenarios. Left: for (4.3) no feasible equilibrium exists for the parameter values $r = 0.9$, $m = 0.3$, $p = 0.9$, $q = 0.3$, $K_p = 10$, $K_q = 10$; the two dots on the axes the two possible system's outcomes, implying the principle of competitive exclusion. Center: (4.5), just one feasible equilibrium E_3^C , for the parameter values $r = 0.9$, $m = 1.8$, $p = 0.9$, $q = 0.3$, $K_p = 10$, $K_q = 10$; Here coexistence is feasible but unstable. Right (4.4) for the parameter values $r = 0.9$, $m = 3$, $p = 0.9$, $q = 0.3$, $K_p = 10$, $K_q = 10$; the three equilibria E_4^C , E_3^C and E_5^C are ordered left to right, for increasing values of their abscissae; E_3 , the point in the middle, becomes stable, while the new arising points to its left and right, E_4^C and E_5^C , are unstable. In all the frames, the blue continuous line denotes the population $X(\tau) = \sqrt{Q(t)K_Q^{-1}}$ nullcline, while the red dashed line shows the population $Y(\tau) = \sqrt{P(t)K_P^{-1}}$ nullcline, with variable transformations indicated in the Appendix A0.

275 pitchfork and saddle-node bifurcation. It is important to mention here that the proofs of desired lo-
 276 cal bifurcations can not be provided with the model (4.1). To prove the fulfilment of the conditions
 277 required for the local bifurcations, we thus rather need to consider a transformed model. In what
 278 follows we just describe the possible bifurcations, while the detailed proofs of their occurrence are
 279 provided at the appendix A5.

280 We investigate first the generation of the interior equilibrium point from the trivial equilibrium
 281 point $(0, 0)$ through a pitchfork bifurcation. We consider the model (4.1), fix the parameter values
 282 $r = 0.9$; $K_Q = 10$; $q = 0.3$; $K_P = 10$; $p = 0.9$ and let m be the bifurcation parameter. For
 283 $m = 0.3$, two non-trivial nullclines of (4.1) are tangent to each other at $(0, 0)$ and we find at least
 284 one interior equilibrium point for $m > 0.3$. One interior equilibrium point is generated through
 285 a pitchfork bifurcation, another one is not relevant as its components fail to satisfy the feasibility
 286 condition. This pitchfork bifurcation threshold is denoted by m_{PF} .

287 We investigate first the generation of the interior equilibrium point from the trivial equilibrium
 288 point $(0, 0)$ through a pitchfork bifurcation. The system (4.1) possesses only one interior equilib-
 289 rium point for the above mentioned parameter values in the range $m_{PF} < m < 2.059 \equiv m_{SN}$.
 290 It has instead three interior equilibrium points, with both components positive, for $m > m_{SN}$.
 291 These two new interior equilibrium points are generated through a saddle-node bifurcation at
 292 $m = 2.059 \equiv m_{SN}$. For $r = 0.9$, $K_Q = 10$, $q = 0.3$, $K_P = 10$, $p = 0.9$ and $m = 2.059 = m_{SN}$,
 293 we find one equilibrium point at $E_1(1.196374618, 8.345124260)$ and two coincident equilibrium

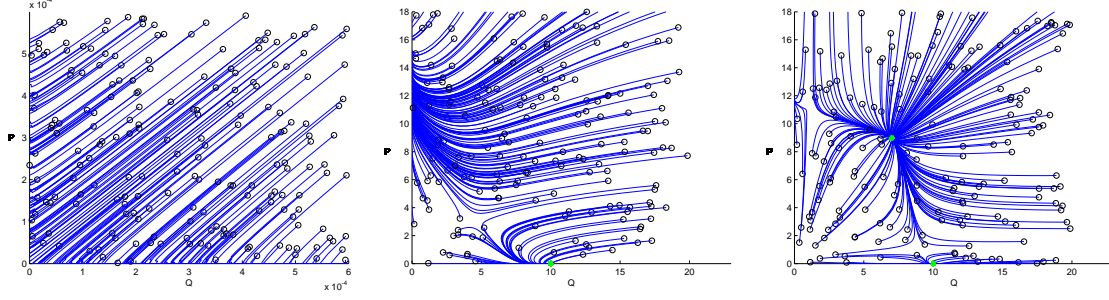


Figure 3: The three possible populations behaviors. Left: the origin is stable, both populations get extinguished; achieved with parameter values $r = 2$, $m = 2$, $p = 33$, $q = 33$, $K_p = 4$, $K_q = 3$ and 200 randomly generated initial conditions, represented by the empty red circles. Note that this occurs also at finite time, when trajectories do not go directly to the origin, but end up on the coordinate axes and then follow them until the origin. Center: bistability and competitive exclusion, only one population survives; achieved with parameter values $r = 0.8888$, $m = 0.602$, $p = 0.401$, $q = 0.5998$, $K_p = 16.5$, $K_q = 10$ and 200 randomly generated initial conditions. Right: tristability, either one population only survives, or the other one, or both together; achieved with parameter values $r = 0.7895$, $m = 0.7885$, $p = 0.225$, $q = 0.2085$, $K_p = 12$, $K_q = 10$ and 200 randomly generated initial conditions. The green full dots, two on the two coordinate axis and one in the first quadrant represent instead the stable equilibria.

294 points $E_*(7.681094754, 3.717334465)$. The pitchfork and saddle-node bifurcation scenario are
 295 shown in Fig. 4 (left).

296 Depending upon the magnitude of the parameters, we can observe the occurrence of two con-
 297 secutive saddle-node bifurcations. As a result we obtain one coexisting equilibrium point for two
 298 disjoint sets of parameter values and in between we find three interior equilibria. To make this
 299 idea more clear, we choose $r = 0.5$; $K_Q = 10$; $q = 0.3$; $K_P = 6$; $p = 0.9$ and let m be the
 300 bifurcation parameter as before. Here the relevant thresholds are $m_{PF} = 0.54$, $m_{SN_1} = 2.427$,
 301 $m_{SN_2} = 2.7$. We find a unique interior equilibrium point when $m_{PF} < m < m_{SN_1}$ and $c > c_{SN_2}$.
 302 Two more interior equilibrium points are generated through the first saddle-node bifurcation thresh-
 303 old at $m = m_{SN_1}$ and again disappear through the second saddle-node bifurcation at $m = m_{SN_2}$.
 304 These bifurcation scenarios are presented in Fig. 4 (right).

305 5 Discussion

306 5.1 Comparison with the classical cases

307 5.1.1 The predator-prey ecosystems

308 In order to compare these results quantitatively, we consider also the classical model with logistic
 309 correction. This is needed because if we rescale it, since it does not contain the square root terms,

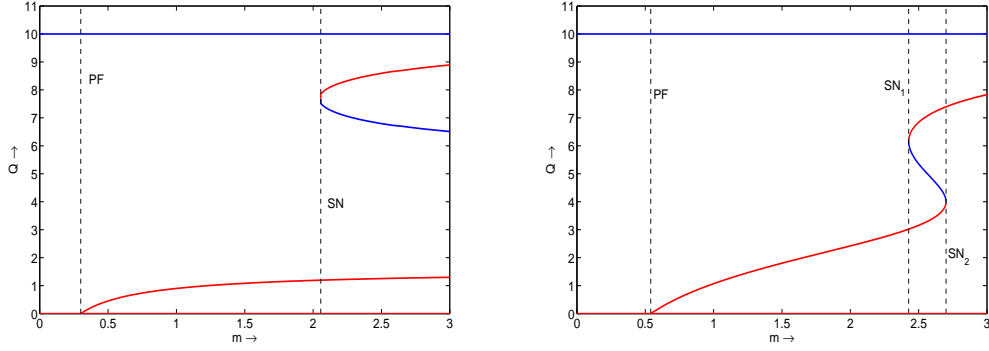


Figure 4: Left: Bifurcation diagram showing the generation of first interior equilibrium point through pitchfork bifurcation followed by the generation of two more interior equilibria through saddle-node bifurcation. Parameter values: $r = 0.9$, $K_Q = 10$, $q = 0.3$, $K_P = 10$, $p = 0.9$. Right: Bifurcation diagram showing the generation of first interior equilibrium point through pitchfork bifurcation followed by the generation and subsequent disappearance of two interior equilibria through two consecutive saddle-node bifurcations. Here the parameter values are $r = 0.5$, $K_Q = 10$, $q = 0.3$, $K_P = 6$, $p = 0.9$.

310 we would find a different adimensionalization, rendering the comparison difficult. Thus we rather
 311 return to the original formulations also for (2.1) and (2.2).

The dimensional form of the coexistence equilibria of the two models (2.1) and (2.2) are (2.4) and (2.5). The dimensional form of the coexistence equilibrium of the classical Lotka-Volterra with logistic correction and of the predator-prey model with individualistic hunting and prey herd behavior, [1], instead are respectively

$$C_* \equiv \left(\frac{m}{p}, \frac{r}{q} \left(1 - \frac{m}{pK} \right) \right), \quad \tilde{E}_2 = \left(\frac{m^2}{p^2}, \frac{mr}{pq} \left(1 - \frac{m^2}{p^2 K} \right) \right).$$

312 At these points, the prey equilibrium values depend only on the system parameters m and p , i.e.
 313 the predators' mortality and predation efficiency. Thus they are independent of their own reproduc-
 314 tive capabilities and of the environment carrying capacity. Further, when the predators' hunting
 315 efficiency is larger than the predators' own mortality, i.e. $m < p$, the equilibrium prey value is
 316 much lower if they gather in herds, i.e. in \tilde{E}_2 , while on the contrary the predators attain instead
 317 higher values, again at \tilde{E}_2 . Conversely, when $m > p$ the prey grouping together, \tilde{E}_2 , allows higher
 318 equilibrium numbers than for their individualistic behavior; the predators instead settle at lower
 319 values if the prey use a defensive strategy, \tilde{E}_2 , and higher ones with individualistic prey behavior,
 320 at C_* .

321 For (2.1) and (2.2), i.e. with coordinated hunting, the equilibrium values involve also the prey
 322 own intrinsic characteristics. In particular for (2.2) the ratio of the predators' hunting efficiency p
 323 versus the square of their mortality m determines if the predators at equilibrium will be more than
 324 the prey, see $E_2^{[ph]}$.

325 A similar result possibly extends for the model of pack hunting coupled with loose, i.e. individ-

326 ualistically behaving, prey, (2.1), but at $E_2^{[pi]}$ the predators population at equilibrium contains the
 327 prey population squared and in principle the latter may not exceed 1, so that the conclusion would
 328 not be immediate. Indeed, at the equilibria $E_2^{[pi]}$ and $E_2^{[ph]}$, the prey populations are the multiplication
 329 of the fractions in the brackets, always smaller than 1, by the carrying capacity K , which may
 330 or not be large. The result could indeed give a population smaller than 1. This in principle is not
 331 a contradiction, because the population need not necessarily be counted by individuals, but rather
 332 its size could be measured by the weight of its biomass.

333 5.1.2 The symbiotic ecosystem

334 We now try to understand how socialization may possibly boost the mutual benefit of the system's
 335 populations.

336 The symbiotic model has always a stable coexistence equilibrium, while in the classical model
 337 the corresponding point \widehat{E}_3^S could be unfeasible, and in such case the trajectories will be un-
 338 bounded. This is biologically questionable, in view of the limited amount of resources available,
 339 However, it shows that in this situation the one-to-one relationship among individuals of different
 340 populations may lead to higher benefits for both of them, than the case in which interactions occur
 341 only through the marginal areas of contact among them.

342 Considering instead only parameters choices where \widehat{E}_3^S is feasible, we compare the resulting
 343 populations levels for the new and the classical model. Taking for both cases $r = 3$, $m = 3$,
 344 $K_Q = 6$, $K_P = 7$, $q = 0.3$, and $p = 0.5$, the behaviors are shown in Figure 5. Starting from the
 same initial conditions, different equilibria are reached.

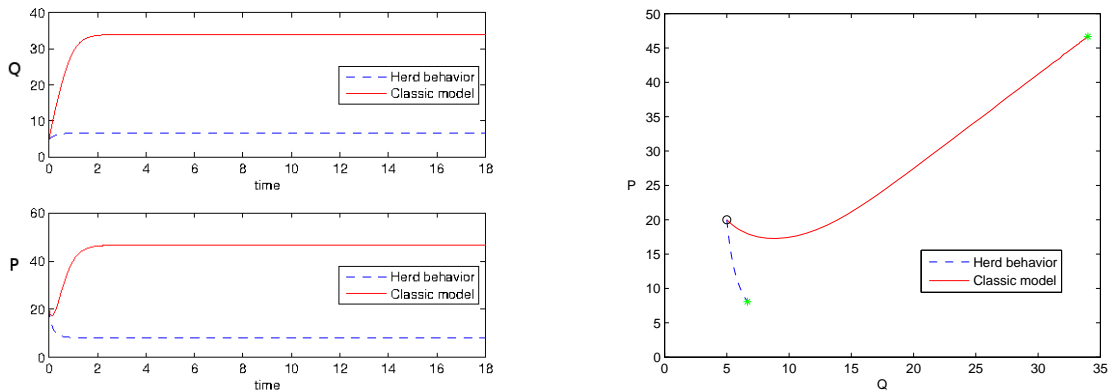


Figure 5: Left: time series of the symbiotic systems (A.19), red continuous, and (3.1), dashed blue, trajectories: top frame Q , bottom frame P ; Right: phase plane for classical (A.19) and new (3.1) symbiotic model. Parameter values: $r = 3$, $m = 3$, $K_Q = 6$, $K_P = 7$, $q = 0.3$, and $p = 0.5$. Trajectories originate from the same initial condition $(5, 20)$. The full green dots represent the final equilibrium values.

345
 346 Clearly the population level is higher in the classical model. The numerical values we obtained
 347 are $Q = 6.66$, $P = 8.06$ for the herd model and $Q = 33.99$, $P = 46.69$ for the classical model.

348 This makes sense, since in symbiotic models the benefit comes from the mutual interactions
 349 between populations. If the latter are scattered in the environment it is more likely for each in-
 350 dividual of one population to get in contact with one of the other. On the other hand, when herd
 351 behaviour is exhibited, only individuals on the outskirts interact with the other population and as
 352 a consequence the innermost individuals receive less benefit since they hardly have the chance to
 353 meet the other population.

354 5.1.3 The competition ecosystem

355 While the classical case exhibits the principle of competitive exclusion, here, instead, we have
 356 found that in the presence of community behavior of both populations, the same occurs, but there
 357 is another possibility, namely tristability. When the conditions arise, the coexistence equilibrium
 358 may be present together with the equilibria in which one population vanishes. Therefore the sys-
 359 tem's outcome is once more determined by the initial conditions, but this time the phase plane
 360 is partitioned into three basins of attractions, corresponding each to one of the possible equilib-
 361 ria. It would be interesting to compute explicitly the boundary of each one of them. For this task
 362 state-of-the-art approximation theoretic algorithms have been devised, [9, 10, 11, 13, 14].

363 We now compare the population levels when a coexistence equilibrium is stable in both clas-
 364 sical and new model. Considering the parameters $r = 2$, $m = 3$, $K_Q = 6$, $K_P = 8$, $q = 0.2$ and
 365 $p = 0.09$, with suitable initial conditions, the behavior of the two models is shown in Figure 6.
 366 From the same initial conditions, trajectories of the two models evolve toward different equilibria.
 The population levels are thus higher in the herd model, at $Q^C = 6.26$ and $P^C = 9.17$ while for

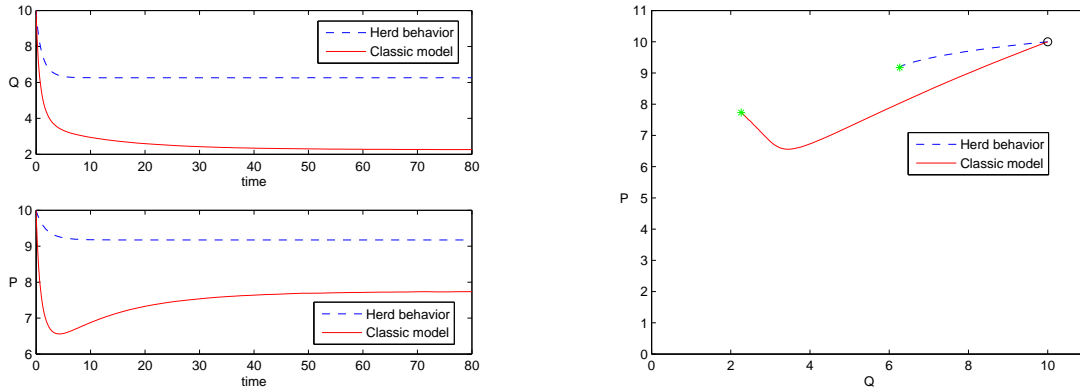


Figure 6: Left: time series of the systems trajectories; Right: phase plane for classical and new competition model. Parameter values: $r = 0.8$, $m = 0.5$, $p = 0.05$, $q = 0.07$, $K_p = 10$, $K_q = 7$. Both trajectories originate from the same initial condition (10, 10). The full green dots represent the equilibrium points.

367 the classic model we find $\tilde{Q}^C = 2.26$ and $\tilde{P}^C = 7.74$. This is not surprising for the same reasons
 368 for which the opposite behavior occurs in the symbiotic models. In herd models, only individuals
 369 at the outskirts meet individual of the other species. This means that individuals at the centre of
 370

371 the flock here receive less harm from the competition. On the contrary, in the classic model, indi-
372 viduals of the two populations are mixed together, so that the whole populations are harmed by the
373 competition.

374 5.2 Conclusions

375 We have presented four models for non-classical population interactions, in that the populations
376 involved in some way exhibit a socialized way of living. This investigation completes the one
377 undertaken in [1], in that all the situations that are possible in terms of individualistic or gathering
378 populations behavior are now analysed. The models missing in [1] are presented here: we allow
379 predators to hunt in packs, as well as both intermingling populations to gather together, in the two
380 cases of symbiosis and competition, so that they interact not on an individualistic basis, but rather
381 in some coordinate fashion.

382 The newly introduced symbiotic model on a qualitative basis behaves like the classical one.
383 The populations settle always at the coexistence equilibrium. Only, their levels are quantitatively
384 smaller than in the classical case since the mutually beneficial interactions in the new model are
385 somewhat reduced.

386 For predator-prey interactions in the presence of predators' pack hunting, we may have the prey
387 behave in herds or individualistically. The most prominent discrepancy between these two cases
388 is the fact that both populations may disappear, under specific unfortunate conditions, when the
389 prey use a defensive coordinate strategy. This does not happen instead if they move loose in the
390 environment, i.e. exhibit individualistic behavior, since they attain a coexistence equilibrium. This
391 finding is quite counterintuitive, because it could imply that the defensive mechanism is ineffective.
392 But an interpretation could be provided, since herds are more easily encountered by predators in
393 their wanderings than individuals who can more easily hide in the terrain configuration. Once the
394 prey herds are completely wiped out, the predators also will disappear, since they are assumed not
395 to be generalist, i.e. their only food source is the prey under consideration. Ecosystem extinction
396 has also been rarely observed in the model without pack predation, [33]. The system with prey
397 herd behavior also shows limit cycles, i.e. the populations can coexist also through persistent
398 oscillations, not only at a stable equilibrium, which instead is the only possible system's outcome
399 for the model with individualistic prey. A similar result had been discovered earlier in case of
400 individualistic predators hunting, [1], constituting the major difference between the prey group
401 defense model with uncoordinated predation and the classical predator-prey system. Finally, on
402 the quantitative side, the coexistence population values for these two models with pack hunting
403 differ, but without specific informations on the parameter values it is not possible to assess which
404 system will provide higher population values.

405 The competition system presented here allows again the extinction of both populations, under
406 unfavorable circumstances, while this never happens for the classical model. Ecosystem disap-
407 pearance occurs when (4.2) holds, a condition that in the nondimensional model is equivalent to

$$a > bc, \tag{5.1}$$

408 as stated in Proposition 15. When the competition system thrives, it does at higher levels for both

409 populations than those achieved in the classical model. Thus in this case populations coordinated
410 behavior boosts their respective sizes, in case the system parameters are in the range for which
411 coexistence occurs.

412 But the major finding in this context of social behavior among all possible populations behav-
413 ior is found for the competition case. Indeed the system in suitable conditions can show the phe-
414 nomenon of competitive exclusion as the classical model does, but in addition we have discovered
415 that both populations can thrive, together with the situations predicted by the competitive exclusion
416 principle. In other words, we have found that the rather simple model (4.1) (or in nondimensional
417 form (A.8)) may exhibit tristability, see once more the right picture in Figure 3. This appears to be
418 a novel and quite interesting finding further characterizing the systems with socialized behaviors.
419 The authors do not know of any other simple related model with such behavior.

420 **Acknowledgment:** The research has been partially supported by the project “Metodi numerici
421 nelle scienze applicate” of the Dipartimento di Matematica “Giuseppe Peano”. The authors thank
422 the referees for their constructive criticism, that helped in reshaping the paper for a better presen-
423 tation of the results.

424 References

- 425 [1] V. Ajraldi, M. Pittavino, E. Venturino, *Modeling herd behavior in population systems*, Non-
426 linear Analysis: Real World Applications, 12 (2011) 2319-2338.
- 427 [2] M. Banerjee, B. W. Kooi, E. Venturino, *An ecoepidemic model with prey herd behavior and*
428 *predator feeding saturation response on both healthy and diseased prey*, Mathematical Mod-
429 els in Natural Phenomena, 12 (2), 133–161, 2017; <https://doi.org/10.1051/mmnp/201712208>
- 430 [3] P.A. Braza, *Predator prey dynamics with square root functional responses*, Nonlinear Analy-
431 sis: Real World Applications, 13 (2012) 1837-1843.
- 432 [4] S. P. Bera, A. Maiti, and G. P. Samanta, *Stochastic analysis of a prey-predator model with*
433 *herd behaviour of prey*, Nonlinear Analysis: Modelling and Control, 21 (3) (2016) 345-361.
- 434 [5] S. P. Bera, A. Maiti, and G. P. Samanta, *Dynamics of a food chain model with herd behaviour*
435 *of the prey*, Model. Earth Syst. Environ., 2(131) (2016) DOI 10.1007/s40808-016-0189-4.
- 436 [6] I. M. Bulai, E. Venturino, *Shape effects on herd behavior in ecological in-*
437 *teracting population models*, Mathematics and Computers in Simulation, 2017.
438 <https://doi.org/10.1016/j.matcom.2017.04.009>
- 439 [7] E. Caccherano, S. Chatterjee, L. Costa Giani, L. Il Grande, T. Romano, G. Visconti, E. Ven-
440 turino, *Models of symbiotic associations in food chains*, in Symbiosis: Evolution, Biology
441 and Ecological Effects, A.F. Camisão and C.C. Pedroso (Editors), Nova Science Publishers,
442 Hauppauge, NY, 189-234, 2012.

- 443 [8] E. Cagliero, E. Venturino, *Ecoepidemics with infected prey in herd defense: the harmless*
444 *and toxic cases*, IJCM, 93(1), 108-127, 2016. doi: 10.1080/00207160.2014.988614. doi:
445 10.1080/00207160.2014.988614.
- 446 [9] R. Cavoretto, A. De Rossi, E. Perracchione, E. Venturino, *Reconstruction of separatrix curves*
447 *and surfaces in squirrels competition models with niche*, Proceedings of the 2013 Interna-
448 tional Conference on Computational and Mathematical Methods in Science and Engineer-
449 ing, I.P. Hamilton, J. Vigo-Aguiar, H. Hadeli, P. Alonso, M.T. De Bustos, M. Demiralp,
450 J.A. Ferreira, A.Q.M. Khaliq, J.a. López-Ramos, P. Oliveira, J.C. Reboredo, M. Van Daele,
451 E. Venturino, J. Whiteman, B. Wade (Editors) Almeria, Spain, June 24th-27th, 2013, v. 3, p.
452 400-411.
- 453 [10] R. Cavoretto, A. De Rossi, E. Perracchione, E. Venturino, *Reliable approximation of sepa-*
454 *ratix manifolds in competition models with safety niches*, International Journal of Computer
455 Mathematics, 92(9), 1826-1837 (2015). <http://dx.doi.org/10.1080/00207160.2013.867955>
- 456 [11] R. Cavoretto, A. De Rossi, E. Perracchione, E. Venturino, *Robust approximation algorithms*
457 *for the detection of attraction basins in dynamical systems*, to appear in Journal of Scientific
458 Computing
- 459 [12] C. Cosner, D.L. DeAngelis, J.S. Ault, D.B. Olson, *Effects of Spatial Grouping on the Func-*
460 *tional Response of Predators*, Theoretical Population Biology, 56, (1999) 65-75.
- 461 [13] E. Francomano, F. M. Hilker, M. Paliaga, E. Venturino, *On basins of attraction for a predator-*
462 *prey model via meshless approximation*, to appear in AIP NUMTA 2016.
- 463 [14] E. Francomano, F. M. Hilker, M. Paliaga, E. Venturino, *An efficient method to reconstruct*
464 *invariant manifolds of saddle points*, to appear in DRNA
- 465 [15] H.I. Freedman, G. Wolkowicz, *Predator-prey systems with group defence: the paradox of*
466 *enrichment revisited*, Bull. Math. Biol., 48 (1986) 493-508.
- 467 [16] S.A.H. Geritz, M. Gyllenberg, *Group defence and the predator's functional response*, Journal
468 of Mathematical Biology 66, (2013) 705-717.
- 469 [17] I. Giardina, *Collective behavior in animal groups: theoretical models and empirical studies*,
470 HFSP J. 2008 August; 2(4): 205-219, doi: 10.2976/1.2961038.
- 471 [18] G. Gimmelli, B. W. Kooi, E. Venturino, *Ecoepidemic models with prey group defense and*
472 *feeding saturation*, Ecological Complexity, 22 (2015) 50-58.
- 473 [19] M. Haque, E. Venturino, *Mathematical models of diseases spreading in symbiotic communi-*
474 *ties*, in J.D. Harris, P.L. Brown (Editors), Wildlife: Destruction, Conservation and Biodiver-
475 sity, NOVA Science Publishers, New York, 2009, 135-179.
- 476 [20] M. J. Harrison, *Signaling in the arbuscular mycorrhizal symbiosis*, Annu. Rev. Microbiol.,
477 59: 19-42, 2005. doi:10.1146/annurev.micro.58.030603.123749, PMID 16153162

- 478 [21] M. P. Hassell, G. C. Varley, *New inductive population model for insect parasites and its*
479 *bearing on biological control*, Nature (London) 223 (1969) 1133-1137.
- 480 [22] B.W. Kooi, E. Venturino, *Ecoepidemic predator-prey model with feeding satiation, prey herd*
481 *behavior and abandoned infected prey*, Math. Biosci., 274 (2016) 58-72.
- 482 [23] A. Maiti, P. Sen, D. Manna, and G.P. Samanta, *A predator-prey system with herd behaviour*
483 *and strong Allee effect*, Nonlinear Dynamics and Systems Theory, 16(1) (2016) 86-101.
- 484 [24] H. Malchow, S. Petrovskii, E. Venturino, *Spatiotemporal patterns in Ecology and Epidemi-*
485 *ology*, CRC, Boca Raton, 2008.
- 486 [25] F. Mavrot, F. Zimmermann, E.M. Vilei, M.P. Ryser-Degiorgis, *Is the development of infec-*
487 *tious keratoconjunctivitis in Alpine ibex and Alpine chamois influenced by topographic fea-*
488 *tures?*, European Journal of Wildlife Research, 58(5), 869-874, 2012.
- 489 [26] P. Nardon, H. Charles, “*Morphological aspects of symbiosis*”, *Symbiosis: Mechanisms*
490 *and Systems*. Dordrecht/Boston/London, Kluwer Academic Publishers, 4: 15–44, 2002.
491 doi:10.1007/0-306-48173-1_2
- 492 [27] S. Paracer, V. Ahmadjian, *Symbiosis: An Introduction to Biological Associations*, Oxford
493 [Oxfordshire]: Oxford University Press, 2000. ISBN 0-19-511806-5
- 494 [28] L. Perko, *Differential Equations and Dynamical Systems*, Springer, New York, 2000.
- 495 [29] J. Sapp, *Evolution by association: a history of symbiosis*, Oxford [Oxfordshire]: Oxford
496 University Press, 1994. ISBN 0-19-508821-2
- 497 [30] A. Schüssler, D. Schwarzott, C. Walker, *A new fungal phylum, the Glom-*
498 *eromycota: phylogeny and evolution*, Mycol. Res., 105 (12): 1413-1421, 2001.
499 doi:10.1017/S0953756201005196
- 500 [31] D.J.T Sumpter, *The principles of collective animal behaviour*, Phil. Trans. R. Soc. B 29, v.
501 361, n. 1465 (2006) 5-22, doi: 10.1098/rstb.2005.1733
- 502 [32] R.K. Trench, J.E. Boyle and D.C. Smith, *The Association between Chloroplasts of Codium*
503 *fragile and the Mollusc Elysia viridis. I. Characteristics of isolated Codium chloroplasts*,
504 *Proceedings of the Royal Society of London. Series B, Biological Sciences* 184 (1074): 51–
505 61, 1973. doi:10.1098/rspb.1973.0030.
- 506 [33] E. Venturino, S. Petrovskii, *Spatiotemporal Behavior of a Prey-Predator System with a Group*
507 *Defense for Prey*, Ecological Complexity, 14 (2013) 37-47.
- 508 [34] P. Waltman, *Competition Models in Population Biology*, SIAM CBMS-NSF Regional Con-
509 ference Series in Applied Mathematics, Philadelphia, 1983.

510 Appendix

511 .1

512 A0 - Preliminary results

513 A0.1 - Extinction in finite time

514 **Proposition 1.** *The system (2.2) admits trajectories for which the prey go to extinction in finite*
 515 *time, if their initial conditions lie in the set (2.8).*

516 *Proof.* We follow with suitable modifications the argument exposed in [33]. From the second
 517 equation in (2.2) we get the differential inequality

$$\frac{dP}{dt} \geq -mP \quad (\text{A.1})$$

518 from which $P(t) \geq \widehat{P}(t) = P_0 \exp(-mt)$, where the function $\widehat{P}(t)$ denotes the solution of the
 519 differential equation corresponding to (A.1), with $\widehat{P}(0) = P(0)$. From the first equation in (2.2)
 520 we have further

$$\frac{dQ}{dt} \leq rQ - q\sqrt{P}\sqrt{Q} \leq rQ - q\sqrt{\widehat{P}}\sqrt{Q}. \quad (\text{A.2})$$

521 Let $\widehat{Q}(t)$ denote the solution of the differential equation obtained from (A.2) using the rightmost
 522 term, with $\widehat{Q}(0) = Q(0)$. It follows that $Q(t) \leq \widehat{Q}(t)$. Using the integrating factor $W(t) =$
 523 $\widehat{Q}(t) \exp(-rt)$, we obtain

$$\sqrt{W(t)} = \sqrt{W(0)} - \frac{q\sqrt{P(0)}}{m+r} h(t), \quad h(t) = \left[1 - \exp\left(-\frac{m+r}{2}t\right) \right], \quad (\text{A.3})$$

with finite extinction time t^* obtained by setting $W(t^*) = 0$, observing that $W(0) = \widehat{Q}(0) = Q(0)$:

$$t^* = -\frac{2}{m+r} \ln \left(1 - \frac{m+r}{q} \sqrt{\frac{Q(0)}{P(0)}} \right).$$

524 The function $h(t)$ in (A.3) is an increasing function of t with $h(0) = 0$, $h(\infty) = 1$, so that there is
 525 a t^* for which $W(t^*) = \widehat{Q}(t^*) = 0$ if and only if

$$\sqrt{W(0)} < \frac{q\sqrt{P(0)}}{m+r}. \quad (\text{A.4})$$

Since $W(0) = Q(0)$, we have $\widehat{Q}(t^*) = 0$ if the following inequality for the initial conditions of the
 trajectories is satisfied,

$$\sqrt{P(0)} > \frac{m+r}{q} \sqrt{W(0)},$$

526 from which the set Ξ given in (2.8) is immediately obtained. □

527 **A0.2 - Models simplification**

528 As remarked in [1], singularities could arise in the system's Jacobian when one or both populations
 529 vanish. This may cause difficulties in the analysis, so that we reformulate the model to avoid them.

530 For the predator-prey cases rescaling for the model (2.1) is obtained through

$$X = \frac{Q}{K}, \quad Y = \frac{q\sqrt{P}}{m}, \quad \tau = mt,$$

531 and defining the new parameters

$$b = \frac{r}{m}, \quad c = \frac{pqK}{2m^2}.$$

532 The adimensionalized system for the pack predation–individual prey model can thus be written as

$$\frac{dX}{d\tau} = b(1 - X)X - XY, \quad \frac{dY}{d\tau} = -\frac{1}{2}Y + cX, \quad (\text{A.5})$$

533 while in the absence of predators, the system reduces just to the first equation. In this case, easily,
 534 the prey follow a logistic growth, toward the adimensionalized carrying capacity $X_1 = 1$.

For (2.2) we have instead

$$X = \sqrt{\frac{Q}{K}}, \quad Y = \frac{q}{2m} \sqrt{\frac{P}{K}}, \quad \tau = mt.$$

Define now the adimensionalized parameters

$$e = \frac{r}{2m}, \quad f = \frac{pq}{4m^2}.$$

535 The adimensionalized system for $Y > 0$ for the pack predation–prey herd ecosystem becomes
 536 finally

$$\frac{dX}{d\tau} = e(1 - X^2)X - Y, \quad \frac{dY}{d\tau} = -\frac{1}{2}Y + fX. \quad (\text{A.6})$$

For both models (3.1) and (4.1) we instead define new variables as follows

$$X(\tau) = \sqrt{\frac{Q(t)}{K_Q}}, \quad Y(\tau) = \sqrt{\frac{P(t)}{K_P}}, \quad \tau = t \frac{q\sqrt{K_P}}{2\sqrt{K_Q}},$$

as well as new adimensionalized parameters

$$a = \frac{K_Q p}{K_P q}, \quad b = \frac{r\sqrt{K_Q}}{q\sqrt{K_P}}, \quad c = \frac{m\sqrt{K_Q}}{q\sqrt{K_P}}.$$

537 The adimensionalized systems read, for the symbiotic case (3.1)

$$\frac{dX}{d\tau} = b(1 - X^2)X + Y, \quad \frac{dY}{d\tau} = c(1 - Y^2)Y + aX, \quad (\text{A.7})$$

538 while for the competing situation (4.1) we find

$$\frac{dX}{d\tau} = b(1 - X^2)X - Y, \quad \frac{dY}{d\tau} = c(1 - Y^2)Y - aX. \quad (\text{A.8})$$

539 All the new adimensionalized parameters are combinations of the old nonnegative parameters
540 r, m, p, q, K ; as a consequence, they must be nonnegative as well.

541 **Remark 2.** *Note that these reformulated group behavior models need a special care in treating*
542 *vanishing populations, because in eliminating the singularity we divide by X and Y , except for X*
543 *in the case (A.5). Therefore all the simplified models (A.7)-(A.6) hold for strictly positive popula-*
544 *tions. If one population vanishes, no information can be gathered by the latter, we rather have to*
545 *turn to the original formulations (3.1)-(4.1).*

546 For the later analysis of the equilibria stability it is imperative to consider the Jacobians of these
547 systems. We find the following matrices respectively, for the predator-prey cases, the Jacobian of
548 (A.5) is

$$J^{PP1} \equiv \begin{pmatrix} b - 2bX - Y & -X \\ c & -\frac{1}{2} \end{pmatrix}, \quad (\text{A.9})$$

549 while the one for (A.6) reads

$$J^{PP2} \equiv \begin{pmatrix} e(1 - 3X^2) & -1 \\ f & -\frac{1}{2} \end{pmatrix}. \quad (\text{A.10})$$

550 Considering the symbiotic and competing situations, for (A.7) we find

$$J^S \equiv \begin{pmatrix} b(1 - 3X^2) & 1 \\ a & c(1 - 3Y^2) \end{pmatrix} \quad (\text{A.11})$$

551 and for (A.8) we have

$$J^C \equiv \begin{pmatrix} b(1 - 3X^2) & -1 \\ -a & c(1 - 3Y^2) \end{pmatrix}. \quad (\text{A.12})$$

552 **A1 - Analysis of predator-prey ecosystems**

553 **A1.1 - Pack predation and individualistic prey behavior**

554 **Proposition 3.** *All positive solutions of the pack predation-individual prey system (A.5) are for-*
555 *ward bounded.*

556 *Proof.* Introducing the environment total population, $Z(\tau) = X(\tau) + Y(\tau)$ and summing the
557 equations in (A.5), we have

$$\frac{dZ}{d\tau} = -\frac{1}{2}Y + cX + bX - bX^2 - XY = -\frac{1}{2}Z + \left(c + b + \frac{1}{2} - bX - Y \right) X.$$

558 Take the maximum of the parabola in X on the right hand side, to obtain

$$\frac{dZ}{d\tau} + \frac{1}{2}Z \leq \left(c + b + \frac{1}{2} - bX\right) X \leq \frac{\left(c + b + \frac{1}{2}\right)^2}{4b} \equiv \bar{M}.$$

The above differential inequality leads to

$$Z(\tau) \leq Z(0)e^{-\frac{1}{2}\tau} + 2\bar{M} \left(1 - e^{-\frac{1}{2}\tau}\right) \leq \max\{Z(0), \bar{M}\} = M.$$

559 Note that the positive quadrant is positively invariant for (A.5). Indeed, the open positive Y
 560 axis is an orbit of system (A.5), thus it cannot be crossed by other system trajectories. The axis
 561 $Y = 0$ from the second equation instead repels trajectories. Because the total population is for-
 562 ward bounded, and in view of the fact that the positive quadrant is positively invariant, also each
 563 individual population X and Y is forward bounded as well. \square

564 **Proposition 4.** *The coexistence equilibrium $E_2^{[pi]}$ (2.4) of the system (2.1) is always locally asymp-*
 565 *totically stable.*

566 *Proof.* If J_2^{PP1} denotes the Jacobian matrix (A.9) evaluated at $E_2^{[pi]}$, the Routh-Hurwitz criterion
 567 gives

$$\det(J_2^{PP1}) = -\frac{1}{2}b + \frac{b^2 + 2bc}{b + 2c} = \frac{1}{2}b > 0, \quad \text{tr}(J_2^{PP1}) = -\frac{1}{2} + b - \frac{2b^2 + 2bc}{b + 2c} = -\frac{2b^2 + 2c + b}{2(b + 2c)} < 0. \quad (\text{A.13})$$

568 Both conditions hold so that the eigenvalues have negative real part and $E_2^{[pi]}$ is always a stable
 569 equilibrium. \square

570 **Remark 5.** *For (A.5) Hopf bifurcations cannot arise at coexistence, since in (A.13) $\text{tr}(J_2^{PP1}) < 0$*
 571 *is a strict inequality.*

572 **Proposition 6.** *The coexistence equilibrium $E_2^{[pi]}$ of the pack predation-individual prey system*
 573 *(A.5) is also globally asymptotically stable in the open positive quadrant.*

574 *Proof.* We know already that the open positive quadrant is positively invariant and the solutions
 575 are forward bounded. Note further that by Dulac's criterion, no limit cycles can arise. Take indeed
 576 $g(X, Y) = (XY)^{-1}$, to get

$$\begin{aligned} \frac{\partial}{\partial X} \left[g(X, Y) \frac{dX}{d\tau} \right] + \frac{\partial}{\partial Y} \left[g(X, Y) \frac{dY}{d\tau} \right] &= \frac{\partial}{\partial X} \left[b(1 - X) \frac{1}{Y} - 1 \right] + \frac{\partial}{\partial Y} \left[-\frac{1}{2X} + \frac{c}{Y} \right] \\ &= -\frac{b}{Y} - \frac{c}{Y^2} < 0. \end{aligned}$$

577 By the Poincaré-Bendixson theorem, global stability follows. \square

578 The phase plane picture also supports these conclusions as well, Figure 7.

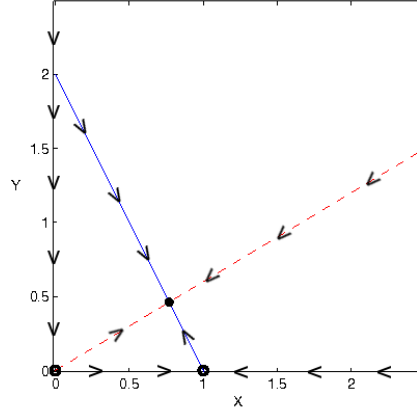


Figure 7: Phase plane sketch of the model (2.1) with parameters values $b = 2$, $c = 0.3$, corresponding to the original parameter values $r = 0.6$, $m = 0.3$, $p = 0.0072$, $q = 1.5$, $K = 5$. Blue continuous line: population X nullcline; red dashed line: population Y nullcline.

579 **A1.2 - Analysis of pack predation and prey herd behavior**

580 **Proposition 7.** *All positive solutions of the pack hunting-prey herd behavior system (A.6) are*
 581 *forward bounded.*

582 *Proof.* First of all, for an arbitrary $k \geq 0$, we have from the first equation in (A.6):

$$\frac{dX}{d\tau} + kX \leq (e + k)X - eX^3 = \varphi(X) \leq \varphi_m, \quad \varphi_m = \varphi(X_m), \quad X_m = \sqrt{\frac{e + k}{3e}},$$

from which

$$X(\tau) \leq \max \{X(0), \varphi_m k^{-1}\} = \tilde{X}.$$

583 Then from the second equation in (A.6) solving the differential inequality we obtain the estimate

$$\frac{dY}{d\tau} \leq -\frac{1}{2}Y + f\tilde{X}, \quad Y(\tau) \leq Y(0)e^{-\frac{1}{2}\tau} + 2f\tilde{X}(1 - e^{-\frac{1}{2}\tau}) \leq \max \{Y(0), 2f\tilde{X}\} = \tilde{Y}. \quad (\text{A.14})$$

Furthermore, from the second equation (A.6) the trajectories are repelled away from the X axis. Recalling that (A.6) holds for $X \neq 0$, using (A.14) in the first equation of (A.6), we can bound X only with a possibly negative value:

$$\frac{dX}{dt} \geq -eX^3 - \tilde{Y} \quad X(t) \geq (et + X(0)^{-2})^{-\frac{1}{2}} - \sqrt[3]{\frac{\tilde{Y}}{3}}.$$

584 In this case, as discussed in Remark 1, if X drops to the value 0, (A.6) is not valid and we need
 585 to return to the original formulation (2.2). But for the latter as remarked in [33], on the Y axis
 586 the differential system does not satisfy the Lipschitz condition, so that uniqueness of the solutions

587 is lost. Technically, there are solutions that drift into the negative X half plane. We need to
 588 understand that they are not biological, and replace them by trajectories moving downwards along
 589 the Y axis to the origin. The ecosystem collapses in finite time, as also remarked in [18, 22, 2]. \square

590 In view of the fact that the ecosystem may disappear in finite time, [18, 22, 2], recall also the
 591 set Ξ given in (2.8), we investigate the stability of the origin in (A.6) as well.

592 **Proposition 8.** *The origin \widehat{E}_0 and coexistence $\widehat{E}_2^{[ph]}$ are the equilibria of the pack hunting-prey*
 593 *herd behavior system (A.6), with population values and feasibility condition given by*

$$\widehat{E}_2^{[ph]} = \left(\widehat{X}_2^{[ph]}, \widehat{Y}_2^{[ph]} \right), \quad \widehat{X}_2^{[ph]} = \sqrt{1 - 2\frac{f}{e}}, \quad \widehat{Y}_2^{[ph]} = 2f\widehat{X}_2^{[ph]}; \quad e \geq 2f. \quad (\text{A.15})$$

594 *There is a transcritical bifurcation with $\widehat{E}_2^{[ph]}$ emanating from \widehat{E}_0 when the parameter e raises up*
 595 *to attain the critical value $e^* = 2f$.*

Proof. The first part of the statement is easy. The characteristic polynomial at the origin \widehat{E}_0 is

$$\lambda^2 + \left(\frac{1}{2} - e \right) \lambda + f - \frac{1}{2}e = 0.$$

596 The Routh-Hurwitz stability conditions for the origin \widehat{E}_0 then become

$$2f > e, \quad e < \frac{1}{2}. \quad (\text{A.16})$$

597 The second claim follows comparing the first inequality in (A.16) with the feasibility condition in
 598 (A.15). In fact, at e^* the origin becomes unstable, while instead $\widehat{E}_2^{[ph]}$ becomes feasible. \square

599 **Proposition 9.** *For the pack hunting-prey herd behavior system (A.6), the equilibrium \widehat{E}_0 when*
 600 *locally asymptotically stable, namely the conditions (A.16) hold, is also globally asymptotically*
 601 *stable in the open positive quadrant.*

602 *Proof.* Since the open positive quadrant is positively invariant and the solutions there forward
 603 bounded, using Dulac's criterion as follows, the existence of cycles is ruled out. This time take
 604 $g(X, Y) = 1$, to get in this case

$$\begin{aligned} \frac{\partial}{\partial X} \left[g(X, Y) \frac{dX}{d\tau} \right] + \frac{\partial}{\partial Y} \left[g(X, Y) \frac{dY}{d\tau} \right] &= \frac{\partial}{\partial X} [e(1 - X^2)X - Y] + \frac{\partial}{\partial Y} \left[-\frac{1}{2}Y + fX \right] \\ &= e - 3eX^2 - \frac{1}{2} < 0, \end{aligned}$$

605 in view of the second local stability condition of the origin, (A.16). \widehat{E}_0 must also be globally
 606 asymptotically stable by the Poincaré-Bendixson theorem. \square

607 **Proposition 10.** *The coexistence equilibrium $\widehat{E}_2^{[ph]}$ of the system (A.6) is a locally asymptotically*
 608 *stable equilibrium if*

$$\text{tr}(\widehat{J}_2^{PP2}) = -2e + 6f - \frac{1}{2} < 0. \quad (\text{A.17})$$

609 *If $e > \max\{\frac{1}{2}, 3f - \frac{1}{4}\}$ (A.17) holds. But if $2f < e < 3f - \frac{1}{4}$ (A.17) is not true and $\widehat{E}_2^{[ph]}$ is*
 610 *unstable.*

611 *Proof.* Let the Jacobian evaluated at $\widehat{E}_2^{[ph]}$ be denoted by \widehat{J}_2^{PP2} . The Routh-Hurwitz conditions are
 612 now $\det(J_2^{PP2}) = e - 2f > 0$, which always holds if the feasibility condition (A.15) is strictly
 613 satisfied, and (A.17). If the latter holds then $\widehat{E}_2^{[ph]}$ is stable. \square

614 Figures 8 and 9 illustrate geometrically the two situations in which $\widehat{E}_2^{[ph]}$ is feasible and when
 615 it is unfeasible. The different possible ecosystem outcomes in the parameter space, corresponding
 616 to the various situations of (A.17), are shown in Figure 10.

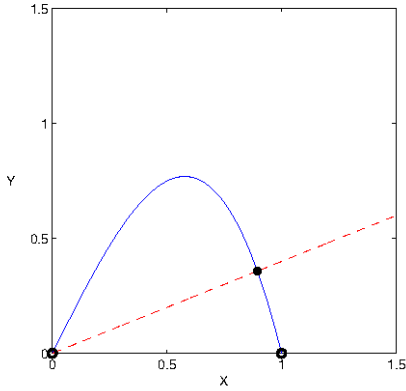


Figure 8: Nullclines of system (A.6) with $e \geq 2f$, both \widehat{E}_0 and $\widehat{E}_2^{[ph]}$ exist. Parameter values: $e = 2$, $f = 0.2$, $r = 0.5$, $m = 0.125$, $p = 0.5$, $q = 0.025$, $K = 10$. Blue continuous line: population X nullcline; red dashed line: population Y nullcline. The full dot indicates the stable equilibrium $\widehat{E}_2^{[ph]}$.

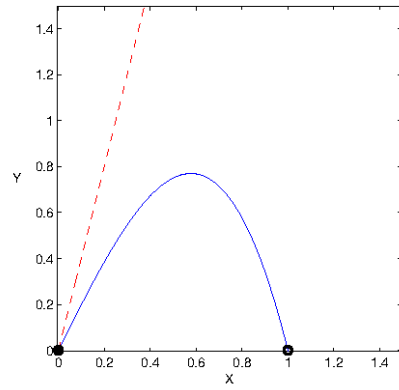


Figure 9: Nullclines of system (A.6) with $e < 2f$, $\widehat{E}_2^{[ph]}$ is unfeasible. Parameter values: $e = 2$, $f = 2.0$, $r = 0.5$, $m = 0.125$, $p = 0.5$, $q = 0.25$, $K = 10$. Blue continuous line: population X nullcline; red dashed line: population Y nullcline. The full dot indicates the stable equilibrium \widehat{E}_0 .

617 **Proposition 11.** *The the pack hunting-prey herd behavior system (A.6) admits a Hopf bifurcation*
 618 *at the coexistence equilibrium $\widehat{E}_2^{[ph]}$ when the bifurcation parameter e crosses the critical value e^\dagger*
 619 *that corresponds to r^\dagger given in (2.7).*

$$e^\dagger = 3f - \frac{1}{4}. \quad (\text{A.18})$$

620 *Proof.* In addition to the transcritical bifurcation of Proposition 8, we show now that special param-
621 eters combinations originate Hopf bifurcations near $\widehat{E}_2^{[ph]}$. Recall that purely imaginary eigenvalues
622 are needed, and this occurs when the trace of the Jacobian vanishes. Thus (A.17) must become an
623 equality and the constant term in the characteristic equation is positive, $\det(\widehat{J}_2^{PP^2}) = e - 2f > 0$.
624 But the latter holds from (A.15). \square

625 Thus the solutions of the system start oscillating in a persistent manner around the coexistence
626 equilibrium when the bifurcation parameter e crosses the critical value e^\dagger , (A.18). This result is
627 observed in Figure 10, where the thick straight line indicates the critical parameter values.

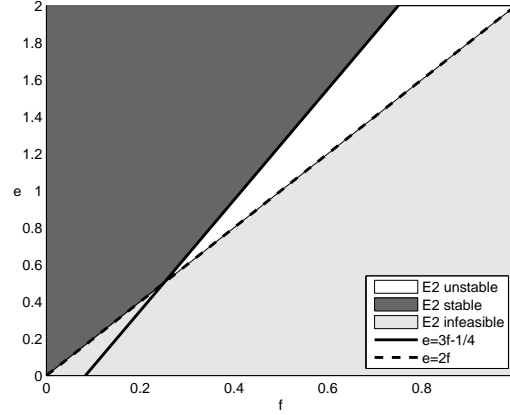


Figure 10: Region of the $f - e$ parameter space in which the coexistence equilibrium of (A.6) is stable.

628 **A3 - Analysis of the symbiotic model**

629 **The classical case**

630 The results of the classical case,

$$\frac{dQ}{dt} = r \left(1 - \frac{Q}{K_Q} \right) Q + qPQ, \quad \frac{dP}{dt} = m \left(1 - \frac{P}{K_P} \right) P + pPQ, \quad (\text{A.19})$$

are summarized in [1]. Extensions of classical symbiotic systems have been recently investigated, to models incorporating diseases [19], or to food chains, [7]. In short, the three equilibria in which at least one population vanishes are unstable, $\widehat{E}_0^S = (0, 0)$, $\widehat{E}_1^S = (K_Q, 0)$ and $\widehat{E}_2^S = (0, K_P)$. The coexistence equilibrium

$$\widehat{E}_3^S = \left(\frac{K_Q m (r + pK_P)}{rm - pqK_P K_Q}, \frac{K_P r (m + qK_Q)}{rm - pqK_P K_Q} \right)$$

631 is unconditionally stable when feasible, i.e. $rm < pqK_P K_Q$. Note that if \widehat{E}_3^S is unfeasible the
 632 trajectories are unbounded, which is biologically scarcely possible in view of the environment's
 633 limited resources.

634 **The herd behavior case**

Looking for the coexistence equilibria, solving for Y the first equation in (A.7) and substituting
 into the second one, we are led to the ninth degree equation

$$X[a - bc(1 - X^2)(1 - b^2 X^6 + 2b^2 X^4 - b^2 X^2)] = 0.$$

635 Factoring out X , the remaining equation is a quartic in X^2 , but still with cumbersome analytic
 636 solutions. However, we can turn to a graphical analysis of the system of equations originated by
 637 (A.7). The coexistence equilibrium will be the intersection of the two cubic functions,

$$Y_s(X) = bX(X^2 - 1), \quad X_s(Y) = \frac{c}{a}Y(Y^2 - 1), \quad (\text{A.20})$$

638 obtained from the equilibrium equations of (A.7).

639 **Proposition 12.** *The coexistence equilibrium of the symbiotic system (A.7) is unique and always*
 640 *feasible.*

641 *Proof.* The two cubic functions (A.20) intersect the axes corresponding to their domains at three
 642 fixed points, 0 and ± 1 . Further, from the largest positive root, they raise up to infinity. Since their
 643 domains are on orthogonal axes, it follows that there always exists a unique positive equilibrium.
 644 □

645 A typical situation is shown in Figure 11 for a choice of hypothetical parameter values. Note
 646 that in this case, there are nine intersections among the two curves Y_s and X_s . For other situations,
 647 some of the intersections in the second and fourth quadrant may disappear. But the origin and
 648 the ones in the first and third quadrants exist always. The intersection in the first quadrant is
 649 feasible, leading to the coexistence equilibrium $E_3^S = (X_3^S, Y_3^S)$. The positive solutions of (A.7)
 650 are forward bounded, as can easily be seen by drawing the system's trajectories, a claim that is also
 651 mathematically rigorously proven in Proposition 14 below.

652 **Proposition 13.** *No Hopf bifurcations can arise at the coexistence equilibrium of the symbiotic*
 653 *system (A.7).*

654 *Proof.* To have Hopf bifurcations, we need purely imaginary eigenvalues. This occurs when the
 655 trace of the Jacobian vanishes and simultaneously the determinant is positive, i.e.

$$b(1 - 3X^2) + c(1 - 3Y^2) = 0, \quad b(1 - 3X^2)c(1 - 3Y^2) - a > 0. \quad (\text{A.21})$$

It can be easily seen that solving for b from the first condition and substituting into the second one,
 we find

$$a < -c^2(1 - 3Y^2)^2 < 0,$$

656 which is a contradiction. □

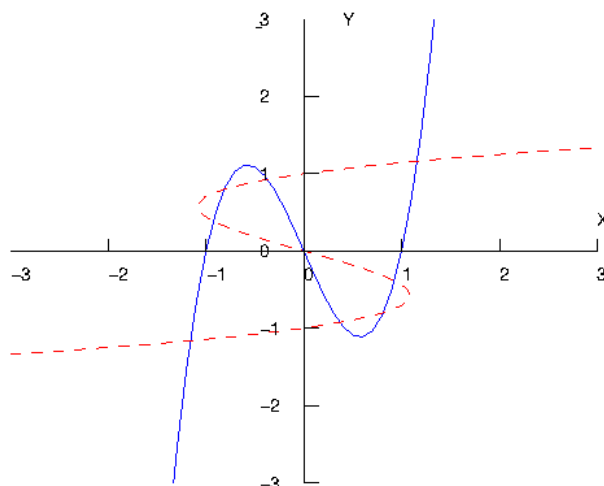


Figure 11: Nullclines of equations system from (A.7). The X nullcline corresponds to the blue continuous curve $Y = Y_s(X)$, conversely The Y nullcline corresponds to the red dashed function $X = X_s(Y)$. The phase plane of interest is obviously only the set $\{(X, Y) : X \geq 0, Y \geq 0\}$. The figure is obtained for the following parameter values $a = 0.6, b = 2.9, c = 1.7, r = 2.9, m = 1.7, p = 0.6, q = 1, K_P = 10, K_Q = 10$.

657 **Proposition 14.** *The positive solutions of (A.7) are forward bounded. Its coexistence equilibrium*
 658 *E_3^S is globally asymptotically stable.*

659 *Proof.* We follow the outline of [1]. It is enough to take a large enough box B in the first quadrant
 660 that contains the coexistence equilibrium.

661 On the vertical and on the horizontal sides we show that the dynamical system's flow enters
 662 into the box. Indeed, take a point $\hat{U} = (\hat{X}, \hat{Y})$ in the phase plane, with $\hat{X} > X_3^S, \hat{Y} > Y_3^S$ and
 663 lying below the isocline $X' = 0$ and above the isocline $Y' = 0$, thus for which the inequalities
 664 $X < X_s$ and $Y < Y_s$ hold. It identifies the rectangle B in the phase plane, with opposite vertex
 665 given by the origin, which is a positively invariant set for the model (A.7). In fact on its vertical
 666 side $Y = \hat{Y}$ we have $Y' < 0$ while instead $X' < 0$ on the horizontal line $X = \hat{X}$, showing that the
 667 flow of (A.7) enters into B on these sides.

668 The axes cannot be crossed, on biological grounds, and mathematically, because both axes
 669 indeed repel the trajectories. Note that in the original situation, however, the square root singularity
 670 in (3.1) prevents the right hand side of the dynamical system to be Lipschitz continuous when the
 671 corresponding population vanishes, so that the assumption for the uniqueness theorem fails on the
 672 axes. But as mentioned in the model formulation, we understand that the differential equations hold
 673 only in the interior of the first quadrant, on the coordinate axes they are replaced by corresponding
 674 equations in which the vanishing population is removed and whose behavior has already been
 675 discussed, leading to equilibria on these axes, either the carrying capacities or the origin.

676 Thus B is a positively invariant set, from which the first claim follows. By the Poincaré-

677 Bendixson theorem, since there are no limit cycles by Proposition 13, the coexistence equilibrium
 678 must be globally asymptotically stable. \square

679 A4 - Analysis of the competition model

680 5.2.1 The classical competition model

681 The classical competition model,

$$\frac{dQ}{dt} = r \left(1 - \frac{Q}{K_Q} \right) Q - qPQ, \quad \frac{dP}{dt} = m \left(1 - \frac{P}{K_P} \right) P - pPQ, \quad (\text{A.22})$$

682 shows under suitable circumstances the competitive exclusion principle. Thus, only one population
 683 survives, while the other one is wiped out. The system's outcome depends only on its initial
 684 conditions, so that if the system has population values lying in the attracting set of one of the
 685 equilibria, the dynamics will be drawn to it unless the environmental conditions, i.e. the parameters
 686 in the model, abruptly change.

687 5.2.2 The herds competition system

688 Although the coexistence equilibria of the competition ecosystem (A.8) could be written as the
 689 roots of the following quartic equation in X^2 ,

$$cb^3 X^8 - 3cb^3 X^6 + 3cb^3 X^4 - cb(b^2 + 1)X^2 - a + cb = 0, \quad (\text{A.23})$$

690 we prefer once more to address the issue by geometrical means since it gives a better interpretation,
 691 treating the problem as an intersection of cubic functions,

$$Y_{[1]}(X) = b(1 - X^2)X, \quad X_{[2]}(Y) = \frac{c}{a}(1 - Y^2)Y. \quad (\text{A.24})$$

692 **Proposition 15.** *No feasible coexistence equilibria for the competing ecosystem (A.8) exist if (5.1)*
 693 *holds. Conversely, at least one feasible equilibrium exists, $E_3^C = (X_3^C, Y_3^C)$. Further, in such case,*
 694 *$b > \frac{3\sqrt{3}}{2}$ and $c > \frac{3\sqrt{3}}{2}a$ are sufficient conditions for three equilibria to exist, i.e. E_4^C , E_3^C and E_5^C ,*
 695 *ordered for increasing values of their abscissae.*

696 *Proof.* Depending on the behavior of the cubic functions (A.24), there could be either three inter-
 697 sections (the origin and one each in the second and fourth quadrants) or five (the previous ones and
 698 one more in the first and third quadrants), or nine. The latter configuration is graphically shown
 699 in Figure 12. The feasible coexistence equilibria are just the intersections in the first quadrant.
 700 Note that no intersections in the first quadrant exist when the slopes at the origin of the two cubic
 701 functions (A.24) satisfy the inequality $Y'_{[1]}(0) < Y'_{[2]}(0)$, the latter denoting of course the inverse
 702 function of $X_{[2]}(Y)$. This condition, rephrased in terms of the parameters, becomes (5.1).

703 Thus, for $a > cb$ there is at most one real positive root, the one corresponding to the intersection
 704 in the fourth quadrant, that is however not feasible, and no intersection exists in the first quadrant,
 705 see the left frame in Figure 2. Thus no coexistence equilibrium arises.

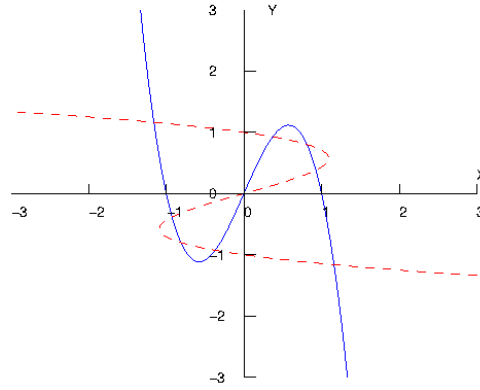


Figure 12: Graphical solution of equations system from (A.8) for the functions $Y_{[1]}(X)$ and $X_{[2]}(Y)$. Parameter values: $a = 0.6$, $b = 2.9$, $c = 1.7$, $r = 2.9$, $m = 1.7$, $p = 0.6$, $q = 1$, $K_p = 10$, $K_q = 10$. Blue continuous line: population X nullcline; red dashed line: population Y nullcline.

706 To better analyse the situation, we apply Descartes' rule of signs to (A.23). There are three sign
 707 variations, since the first four coefficients have alternating signs. The last one must be positive,
 708 because having already ruled out the case (5.1), we are left with $a < cb$. Descartes' rule shows
 709 that in this case there are at most 4 real positive roots. Recall that these roots correspond to the
 710 abscissae of the intersections of the curves (A.24). As discussed above we know that one positive
 711 root corresponds to the intersection that always exists in the fourth quadrant, Figure 12. This
 712 root must then be excluded. As a consequence in this case we have just one or three coexistence
 713 equilibria, see the center and right frames in Figure 2.

Sufficient conditions for three versus one equilibria to exist is that the cubic functions (A.24) have maximum Y -coordinate and X -coordinate respectively in the first quadrant greater than 1. This happens when both the following conditions hold

$$b > \frac{3\sqrt{3}}{2}, \quad c > \frac{3\sqrt{3}}{2}a.$$

714

□

715 **Proposition 16.** *The positive solutions of the competing system (A.8) are forward bounded.*

716 *Proof.* Observe that X decreases when $Y \leq bX(1 - X^2)$ and similarly Y decreases for $X \leq$
 717 $ca^{-1}Y(1 - Y^2)$. This in the phase plane corresponds to having the flow entering a suitable box
 718 Ω^C with one corner in the origin and the opposite one $\Omega_B^C = (X_B, Y_B)$ of size large enough to
 719 contain the vertices of the cubics in all cases of Figure 2. Thus we can take $X_B \geq \max\{1, X_V\}$,
 720 $Y_B \geq \max\{1, Y_V\}$, where X_V and Y_V denote respectively the relative maxima heights of the
 721 cubics. Once more, as found for the pack predation–prey herd behavior model (A.6), here both
 722 axes are not solutions of the system (A.8), but considerations along the lines of those exposed in

723 Proposition 8, in addition to the findings of [18, 22, 2] indicating ecosystem collapse in finite time
 724 in suitable circumstances, can be used. We omit the details. \square

725 **Proposition 17.** *The coexistence equilibria of the competing system (A.8) for which either one of*
 726 *the conditions hold*

$$X < \frac{\sqrt{3}}{3}, \quad Y < \frac{\sqrt{3}}{3}, \quad (\text{A.25})$$

727 namely E_k^C , $k = 4, 5$, are unstable.

728 *Proof.* If both (A.25) hold, the first Routh-Hurwitz condition applied to (A.12) is

$$\text{tr} J^C = b(1 - 3X^2) + c(1 - 3Y^2) < 0. \quad (\text{A.26})$$

729 But for the assumptions (A.25) it cannot be satisfied. If only one of (A.25) is satisfied, say the first
 730 one, from the condition on the trace we obtain $b < -c(1 - 3Y^2)(1 - 3X^2)^{-1}$ and substituting into
 731 the determinant, we have the estimate $\det J^C = b(1 - 3X^2)c(1 - 3Y^2) - a < -c^2(1 - 3Y^2)^2 - a < 0$
 732 so that the second Routh-Hurwitz condition is not satisfied. Hence the claim. \square

733 **Proposition 18.** *The equilibrium E_3^C for which both the following conditions hold*

$$X > \frac{\sqrt{3}}{3}, \quad Y > \frac{\sqrt{3}}{3} \quad (\text{A.27})$$

734 *is stable.*

Proof. The Routh-Hurwitz condition (A.26) easily holds. The second one applied to (A.12) re-
 quires

$$\det J^C = b(1 - 3X^2)c(1 - 3Y^2) - a > 0.$$

735 Observe that the slope of $Y_{[1]}(X)$ is negative at $X = 1$. Hence for the abscissa of E_3^C we must have
 736 $X_3 < 1$. Similarly $Y_3 < 1$, using the slope of $X_{[2]}(Y)$ at $Y = 1$. It follows that $b(1 - 3X^2) > -2b$,
 737 $c(1 - 3Y^2) > -2c$. Thus in turn $\det J^C > 4bc - a$. Since we are in the case $a < bc$, $\det J^C > 0$
 738 follows. \square

739 **Remark 19.** *Upon returning to the original variables, conditions (A.25) and (A.27) respectively*
 740 *become (4.6) and (4.7).*

741 **Remark 20.** *There is thus a subcritical pitchfork bifurcation for which from the unstable E_3^C three*
 742 *equilibria arise, with the equilibrium E_3^C becoming stable and the other ones being unstable.*

743 **Remark 21.** *No Hopf bifurcations arise in this model as they do not in the symbiotic one. Using the*
 744 *same technique as in the proof of Proposition 14, the condition on the trace becomes an equality,*
 745 *so that by solving it for b we get $b = -c(1 - 3Y^2)(1 - 3X^2)^{-1}$. Substituting into the second*
 746 *Routh-Hurwitz condition $\det J^C > 0$, we obtain the contradiction $-c^2(1 - 3Y^2)^2 - a > 0$.*

747 **A5 - Proof of bifurcations**

For the proofs, we follow the approach and the notations of [28]. To prove that the transversality conditions are satisfied by the model (4.1) at the pitchfork and saddle-node bifurcation thresholds respectively, using the original model (4.1), the calculations cannot be performed because they need the first and second order partial derivatives of \sqrt{P} and \sqrt{Q} with respect to P and Q evaluated at $(0, 0)$. We therefore need to work on the suitably modified dimensionless version. For this purpose, we use the transformations

$$x(\sigma) = \sqrt{\frac{Q(t)}{K_Q}}, \quad y(\sigma) = \sqrt{\frac{P(t)}{K_P}}, \quad \sigma = t \frac{q}{2} \sqrt{\frac{K_P}{K_Q}}$$

748 and obtain the following transformed system

$$\frac{dx}{d\sigma} = b(1 - x^2)x - y, \quad \frac{dy}{d\sigma} = c(1 - y^2)y - ax, \quad (\text{A.28})$$

where

$$a = \frac{K_Q p}{K_P q}, \quad b = \frac{r \sqrt{K_Q}}{q \sqrt{K_P}}, \quad b = \frac{r \sqrt{K_Q}}{q \sqrt{K_P}}.$$

749 **A5.1 - Proof of the pitchfork bifurcation**

750 Using the parameter transformations and the parameter values $r = 0.9$, $K_Q = 10$, $q = 0.3$,
 751 $K_P = 10$, $p = 0.9$, $m_{PF} = 0.3$ we obtain $a = 3$, $b = 3$ and $c_{PF} = 1$ as the pitchfork bifurcation
 752 threshold. To verify the transversality conditions for the pitchfork bifurcation we first calculate the
 753 Jacobian matrix for the system (A.28) around $(0, 0)$ at the threshold $c_{PF} = 1$, and find

$$A = \begin{bmatrix} 3 & -1 \\ -3 & 1 \end{bmatrix}.$$

754 The eigenvectors corresponding to the zero eigenvalues of the matrix A and A^t are given by $v =$
 755 $[1, 3]^t$ and $w = [1, 1]^t$ respectively. Let $f = [f_1, f_2]^t$, with $f_1 = b(1 - x^2)x - y$, $f_2 = c(1 - y^2)y - ax$.
 756 We can now perform the following calculations:

$$f_c = \begin{bmatrix} \frac{\partial f_1}{\partial c} \\ \frac{\partial f_2}{\partial c} \end{bmatrix} = \begin{bmatrix} 0 \\ y(1 - y^2) \end{bmatrix} \equiv \begin{bmatrix} F_1 \\ F_2 \end{bmatrix}, \quad Df_c = \begin{bmatrix} \frac{\partial F_1}{\partial x} & \frac{\partial F_1}{\partial y} \\ \frac{\partial F_2}{\partial x} & \frac{\partial F_2}{\partial y} \end{bmatrix} = \begin{bmatrix} 0 & 0 \\ 0 & 1 - 3y^2 \end{bmatrix}.$$

757 We further obtain

$$w^t f_c((0, 0), c_{PF}) = [1, 1] \begin{bmatrix} 0 \\ 0 \end{bmatrix} = 0,$$

758

$$w^t [Df_c((0, 0), c_{PF})v] = [1, 1] \begin{bmatrix} 0 & 0 \\ 0 & 1 \end{bmatrix} \begin{bmatrix} 1 \\ 3 \end{bmatrix} = 3 \neq 0.$$

759 Further,

$$\frac{\partial^2 f_1}{\partial x^2} = -6bx, \quad \frac{\partial^2 f_1}{\partial x \partial y} = 0, \quad \frac{\partial^2 f_1}{\partial y^2} = 0, \quad \frac{\partial^2 f_2}{\partial x^2} = 0, \quad \frac{\partial^2 f_2}{\partial x \partial y} = 0, \quad \frac{\partial^2 f_2}{\partial y^2} = -6cy,$$

760 and hence

$$w^t [D^2 f((0, 0), c_{PF})(v, v)] = w^t \left[\begin{array}{c} \frac{\partial^2 f_1}{\partial x^2} v_1^2 + 2 \frac{\partial^2 f_1}{\partial x \partial y} v_1 v_2 + \frac{\partial^2 f_1}{\partial y^2} v_2^2 \\ \frac{\partial^2 f_2}{\partial x^2} v_1^2 + 2 \frac{\partial^2 f_2}{\partial x \partial y} v_1 v_2 + \frac{\partial^2 f_2}{\partial y^2} v_2^2 \end{array} \right]_{x=0, y=0, c=c_{PF}} = 0.$$

761 Similarly we find

$$\begin{aligned} w^t [D^3 f((0, 0), c_{PF})(v, v, v)] &= w^t \left[\begin{array}{c} \frac{\partial^3 f_1}{\partial x^3} v_1^3 + 3 \frac{\partial^3 f_1}{\partial x^2 \partial y} v_1^2 v_2 + 3 \frac{\partial^3 f_1}{\partial x \partial y^2} v_1 v_2^2 + \frac{\partial^3 f_1}{\partial y^3} v_2^3 \\ \frac{\partial^3 f_2}{\partial x^3} v_1^3 + 3 \frac{\partial^3 f_2}{\partial x^2 \partial y} v_1^2 v_2 + 3 \frac{\partial^3 f_2}{\partial x \partial y^2} v_1 v_2^2 + \frac{\partial^3 f_2}{\partial y^3} v_2^3 \end{array} \right]_{x=0, y=0, c=c_{PF}}, \\ &= [1, 1]^t \left[\begin{array}{c} (-18).1^3 + 3.0.1^2.3 + 3.0.1.3^2 + 0.3^3 \\ 0.1^3 + 3.0.1^2.3 + 3.0.1.3^2 + (-6).3^3 \end{array} \right] = -180 \neq 0. \end{aligned}$$

762 Hence the transversality conditions for the pitchfork bifurcation are satisfied.

763 A5.2 - Proof of the saddle-node bifurcation

764 For $a = 3$, $b = 3$ and $c = 6.8639$ we find an equilibrium point $E_1(0.3459, 0.9135)$ and two
765 coincident equilibrium points $E_*(0.8767, 0.6087)$. The system (A.28) undergoes a saddle-node
766 bifurcation at E_* . Calculating the Jacobian matrix for (A.28) at E_* , we obtain

$$B = \begin{bmatrix} -3.917 & -1 \\ -3 & -0.7659 \end{bmatrix}.$$

767 The eigenvectors corresponding to the zero eigenvalues of B and B^t are given by are $[0.269, -1.0536]^t$
768 and $[0.6612, -0.8633]^t$ respectively.

769 Now we can proceed with the calculations:

$$w^t f_c(E_*, c_{SN}) = [0.6612, -0.8633] \begin{bmatrix} 0 \\ 0.3832 \end{bmatrix} = -0.3308 \neq 0,$$

770

$$\begin{aligned} w^t [D^2 f(E_*, c_{SN})(v, v)] &= \begin{bmatrix} 0.6612 \\ -0.8633 \end{bmatrix}^t \begin{bmatrix} -6.3.(0.8767).(0.269)^2 + 2.0.v_1 v_2 + 0.v_2^2 \\ 0.v_1^2 + 2.0.v_1 v_2 - 6.(6.8639).(0.6087).(-1.054)^2 \end{bmatrix} \\ &= 23.2681 \neq 0. \end{aligned}$$

771 Hence both the transversality conditions for the saddle-node bifurcation are satisfied.